DYNAMIC RESPONSE – TIED ARCH BRIDGES, U.S. 59 HOUSTON

by

Partha P. Sarkar

W. Pennington Vann

Phillip T. Nash

Kishor C. Mehta

J. Walt Oler

Interim Research Report Number 7-1982-1

1. Report No. 7-1982-1	2. Government Accession No.	3. Recipient's Catalog No.
4. Title and Subtitle Dynamic Response - Tied Arch Bridges, U.S. 59 Houston		5. Report Date Revised JUNE 1994 February 1994
		6. Performing Organization Code
7. Author(s) Partha P. Sarkar, W. Pennington Vann, Phillip T. Nash, Kishor C. Mehta, J. Walt Oler		8. Performing Organization Report No.
9. Performing Organization Name and Address Department of Civil Engineering Texas Tech University Box 41023 Lubbock, TX 79409-1023		10. Work Unit No. (TRAIS)
		11. Contract or Grant No. 7-1982
12. Sponsoring Agency Name and Address Texas Dept. of Transportation Research and Technology Transfer Office P.O. Box 5080 Austin, TX 78763		13. Type of Report and Period Covered Interim Sept. 1993 - Jan. 1994
		14. Sponsoring Agency Code

15. Supplementary Notes

16. Abstract

The purpose of this study is to assess the sensitivity of four highway bridges to wind and live loadings. The bridges are planned for construction on U.S. 59 in Houston, Texas. Each bridge will be of the tied-arch type and will be constructed on-grade over cut areas with clear spans in excess of 200 feet (61 m). To expedite construction, unique procedures are planned which use existing bridges as platforms for final fabrication of the tied arches. This procedure requires consideration of wind loading on the arches during construction.

In this study, the bridge design is analyzed under the expected wind loadings based on assumed aerodynamic parameters and the bridge details furnished by the Texas Department of Transportation. A geometrically-scaled wind tunnel model of a typical bridge has been built and tests are in progress to determine the actual aerodynamic parameters. The wind tunnel test results and the traffic loading results will be presented in the next interim report. The analytical study shows that the completed bridge is aerodynamically stable and will not have any major problems due to dynamic vibrations. The same is true for the partially constructed state where the two arches are braced together without the deck. Vortex shedding excitation emerged as more critical than buffeting excitation of the deck and, therefore, it is being more closely examined. A more thorough investigation with the results from the wind tunnel tests will reinforce these results.

17. Key Words Wind loadings, dynamic analyses, vortex shedding, buffeting, Flutter, highway bridges, wind tunnel testing	18. Distribution Statement NO RESTRICTIONS This document is available to the public through the National Technical Information Service, Springfield, VA 22161		
19. Security Classif. (of this report) UNCLASSIFIED	20. Security Classif. (of this page) UNCLASSIFIED	21. No. of Pages 69	22. Price

Form DOT F 1700.7 (8-72)   Reproduction of completed page authorized

TABLE OF CONTENTS

SUMMARY

The purpose of this study is to assess the sensitivity of four highway bridges to wind and live loadings. Each bridge will be constructed on-grade over cut areas with clear spans in excess of 200 feet (61 m). To expedite construction, unique erection procedures are planned which use the existing bridges as platforms for final fabrication of the tied arches. Final designs and erection plans require consideration of possible vibrations induced by wind or traffic loadings. In this study, the bridge design is analyzed under expected wind loading. Structural descriptions include the final configuration and the tied arches without the deck during erection. Laboratory testing of a geometrically-scaled bridge model will provide information on aerodynamic parameters required for predicting wind loads. The present study is done with assumed sets of aerodynamic parameters obtained from the literature.

Findings from the analytical results so far indicate that the peak dynamic stress ranges due to buffeting from a turbulent wind with a basic wind speed of 90-mph (40 m/s) acting perpendicular to the completed bridge would only be of the order of 2 ksi (67 MPa). Stresses of this magnitude should not create fatigue problems in the completed bridge. For the stage of partial construction when the existing bridge has been removed but the new deck has not been installed, the buffeting stress ranges could be considerably larger (up to 12 ksi) in the temporary horizontal braces chosen, but there still should be no fatigue problem because of the very short time when this stage of construction can be subjected to the wind. Dynamic stresses due to moving traffic loads have not yet been determined.

The flutter analysis of the deck shows that the deck without the traffic signs is aeroelastically stable. It is anticipated that the deck with the traffic signs will be more vulnerable than the one without the traffic signs. However, the lower bound of the flutter speed based upon available data from the literature for bridges without signs is calculated as 114 mph (50.7 m/s) which is higher than the basic wind speed for design (90 mph or 40 m/s). Flutter is an instability phenomenon and needs to be avoided for any bridge deck configuration either with or without traffic signs and, therefore, deck stresses due to flutter are never considered in design.

Due to vortex-shedding excitation and buffeting maximum excursions of the deck response in vertical deflection and angular rotation from the position of static equilibrium are calculated for a 96 % confidence limit. The vortex-shedding excitation of the deck seems to be more critical than the buffeting response for the assumed lower bound damping ratio of 0.5%. The maximum excursion of vertical deck response due to vortex shedding is calculated as 1.06 ft (0.32 m) which is a conservative (high) estimate. The vortex-shedding excitation may occur at a wind speed of 29.2 mph (13.1 m/s). The maximum excursions of the vertical deck response and the torsional deck response due to buffeting corresponding to the basic wind speed of the deck (90 mph or 40 m/s) are calculated as 0.31 ft (0.09 m) and 0.0012 radians, respectively. Both the vortex-shedding response and the buffeting response will reduce if the actual damping of the bridge deck is higher than that assumed.

The vibration of the bridge hangers does not seem to pose a potential problem. The wind-tunnel section model of the bridge is complete and the experiments are in progress to find the parameters required for the detailed analyses.

IMPLEMENTATION STATEMENT

Analytical and experimental results will provide guidance for final bridge designs and erection procedures. Field testing of the bridges during and following construction will provide additional information to verify the results of the analyses and laboratory experiments.

LIST OF TABLES

LIST OF FIGURES

1. Introduction

Four highway bridges are planned for construction on U.S. 59 in Houston, Texas. The four bridges will cross U.S. 59 at Hazard, Woodhead, Dunlavy, and Mandell streets. Bridges existing at those locations (see Figure 1.1) have piers in the middle and vertical clearances above U.S. 59 of approximately 14.5 feet (4.4 m). Clearances must be increased to 16.5 feet (5.03 m) and intermediate piers must be eliminated so that the existing medians can become high occupancy vehicle (HOV) lanes. Thus the bridge spans will be roughly doubled, further increasing the demand on the structural systems supporting the prestressed decks. The surface elevation of U.S. 59 cannot be lowered because of a 72-inch (1.83 m) diameter storm sewer under the present bridges.

The storm sewer is required to prevent flooding and its removal would create the need for two additional pumping stations. At the bridge locations, U.S. 59 lacks sufficient width to accommodate traffic during removal of the existing bridges. In addition, the bridge surface levels cannot be raised appreciably because of their need to connect to existing city streets, driveways and buildings. In order to increase the clearances and keep the surface levels roughly the same, the depths of the structures need to be decreased. Virtually the only design option is a variable depth, two-way prestressed slab supported from above the deck.

The support of the deck can be accomplished by one of the following systems: spline beams, trusses, arches, cable stays, or suspension cables. Cable stays and suspension cables have been eliminated because there are no feasible locations for the towers and tie backs. Of the remaining structural options, arches have been selected on the basis of aesthetics. In summary, the arches are needed to provide a bridge with an effective deck depth of 1 foot (0.305 m) and a simple span of 228 feet (69.5 m) that can be built over traffic with a minimum time of closure of the lanes below.

The vibrational characteristics of long-span bridges make them particularly sensitive to wind and live loadings. Depending upon the dynamic characteristics of the bridge, wind loads can affect individual elements or the structure as a whole. Vortex shedding around individual elements can induce vibration and consequent fatigue failure of elements such as hangers. Buffeting wind loads can cause horizontal, vertical or torsional vibrations of major portions of tied arch bridges. Wind loadings

1

are critical both during and after construction. Similarly, live loadings from bridge traffic can create vibration of the bridge structure and its elements. Vibrations depend upon the dynamic characteristics of the bridge structure and the frequencies of the wind and live loads. Loadings in near-phase with the bridge dynamic responses can lead to element fatigue or excessive movements of the bridge. By identifying the expected wind and live loadings, the dynamic characteristics of the bridge can be designed or altered to mitigate undesirable dynamic responses.

2. Problem Statement

Each of the four bridges which are planned for construction on U.S. 59 in Houston, Texas will be on-grade over cut areas with clear spans of 228 feet (69.5 m). The long spans of the bridges increase their susceptibility to vibration problems from wind or live loads. Vibrations from wind loads are a concern during bridge erection and after completion. The bridge designs are tied arches and designs of components and appurtenances to the bridges are not final. Changes in designs can affect wind loads from buffeting or vortex shedding. Other bridges of similar design have experienced vibration problems in hanger elements. Analytical assessments, including laboratory experiments, are needed to determine possible wind loadings and vibrational characteristics of the bridge under wind and live loadings. If vibration problems are discovered, mitigation strategies should be designed with subsequent field testing during construction.

3. Objectives of the Study

The central objective of the present study, as indicated earlier, is to determine if there are potential problems with the tied arch bridge design due to wind loads. A secondary objective is to analyze the bridge dynamically under moving traffic loads. In both cases the dynamics of the bridge are important; TxDOT has already checked the design for 75 psf (3.6 kPa) static wind loading. The types of wind effects that will have been considered by the completion of this project are:

- static wind loading (the steady state response to the mean wind)

- buffeting (dynamic response to turbulence in the wind)

- vortex shedding by the deck

- aeroelastic instability (flutter) and

- hanger vibration due to vortex shedding

For a thorough check of possible problems, some of these analyses will be carried out for the bridge in a critical stage of its construction as well as in its final configuration.

The project includes both experimental and analytical studies. Experiments on a section of the bridge deck in the Texas Tech wind tunnel will verify whether or not there are potential problems regarding vortex shedding, buffeting and/or aeroelastic instability (flutter). Another experiment will attempt to provide a check on the amplitude of cable vibration that can be anticipated. Analytical studies will include finite element computations of the static response of the bridge to the wind loading, determination of the lowest natural frequencies and modes of vibration, and computation of the bridge's dynamic response to wind buffeting, vortex shedding, and traffic loading.

4. Bridge Designs

The tied arch bridges that will replace four existing bridges over U.S. 59 have been designed by the Bridge Division of the Houston Office of the Texas Department of Transportation. A model of the tied arch bridge which has been built by the Texas Department of Transportation is shown in Figure 4.1. Only the basic features of the bridges are presented here to help the reader understand the contents of this report. People other than those in the above office who desire further details can obtain them from the Department of Transportation.

Department of Transportation plan and elevation drawings for one bridge are shown in Figure 4.2. The bridge is 228 ft (69.5 m) long and has a 40 ft (12.2 m) rise from the line joining the end support points to the center of the arch at midspan. There is also a small rise of 1.5 ft (0.46 m) in the deck from the ends to midspan. The deck hangs from the arch from nine double wire ropes that are equally spaced along the span. The steel superstructure of each arch, including the steel construction beam and all the cables, will be constructed on the deck of the existing bridge, hoisted into position on its end supports, and cross-braced to the other arch before the existing bridge is demolished.

Department of Transportation drawings of the cross-section of the deck are shown

in Figure 4.2. Including the overlay, the deck varies in thickness from 12 inches (305 mm) to 17.25 inches (438 mm). The full width of the deck is 60 feet (18.3 m), and it extends 7.5 feet (2.29 m) outside the centerline of each arch to provide a pedestrian walkway. The precast concrete units will be hung from steel construction beams as shown and then grouted and post-tensioned. Then the construction beams are post-tensioned and encased in concrete. The final step will be placement of the overlay on the precast deck units.

5. Terrain and Expected Wind Loadings

Exposure B (Urban and Suburban area, ASCE 1990) is assumed for the terrain over which the wind approaches the bridge. An aerial view in the vicinity of the existing bridges is shown in Figure 5.1 which shows a typical suburban surrounding. The design windspeed is taken as being able to approaching the bridge from any possible direction, and the worst case of its approaching the bridge broadside is taken in most of the calculations. There is no "prevailing wind direction" to be considered when dealing with maximum extreme winds.

Empirical formulae of the wind spectra $S_{uu}(z,n)$ for the along-wind turbulence component u and $S_{ww}(z,n)$ for the vertical-wind turbulence component w at any height z are assumed as follows (Simiu and Scanlan 1986):

$$\frac{n S_{uu}(z,n)}{u_*^2} = \frac{200f}{(1+50f)^{5/3}}, \quad \text{Kaimal Spectrum} \tag{1}$$

$$\frac{n S_{ww}(z,n)}{u_*^2} = \frac{3.36f}{1+10f^{5/3}}, \quad \text{Lumley and Panofsky Spectrum} \tag{2}$$

where
$f = nz/U$, n = frequency in Hz, z = height in ft, U = mean wind speed in ft/s, u_* = friction velocity in ft/s. u_* can be calculated using the mean square value of u $(\overline{u^2})$ which is equal to βu_*^2 where β is assumed as 4.85 to correspond to a densely built-up suburban terrain in the present case. Usually, $I_u(z) = \frac{\overline{u^2(z)}^{1/2}}{U(z)}$ = turbulence intensity of the u component is assumed for calculating u_*.

Calculations are made for the deck with two values of $I_u(z)$, i.e., 25% and 40%, and for the arch with one value of $I_u(z) = 25\%$. The turbulence intensity $I_w(z)$ of the w component is normally $0.3I_u(z)$. Since the deck is nearer to the ground it will be

4

subjected to higher turbulence. In the wind velocity calculation the height z of the deck from the ground is assumed as 16.5 ft (5.03 m) and the height of the arch from the ground is taken as 57.0 ft (17.4 m). The actual height of the arch from the ground varies but the maximum value of the height is considered for conservative results. Later in this report a numerical time-domain analysis with the finite element model is used to calculate the buffeting response of the deck and the arch in the lateral direction.

The design codes for wind loads are based on steady-state wind loads. The effects of fluctuations in the wind and dynamic characteristic of the structure are accounted for in the wind design codes through gust response factors. Since turbulence and dynamics are already accounted for in the buffeting analysis, the gust response factor is dropped from the code formulae for calculating the equivalent design wind speed. The following calculations show the derivation of the mean wind speeds U used for the deck and the arch for the buffeting analysis as referenced in the ASCE 1990 code, the wind design code. Later the wind pressure values are compared with those used by TxDOT as per AASHTO (75 psf or 3.6 kPa).

$$q_z = 0.00256 K_z (IV)^2 = \tfrac{1}{2}\rho U^2 \tag{3}$$

$$P = q_z G_h C_f = \tfrac{1}{2}\rho U^2 G_h C_f \tag{4}$$

where q_z is the velocity pressure; K_z is the exposure coefficient which is a function of height and exposure type; I is the importance factor which depends upon the importance of the structure; V is the basic design wind speed in mph for a 50-year return period at $z = 33$ ft (10.0 m); P is the design wind pressure; G_h is the gust response factor, which is a function of wind turbulence and the dynamic characteristics of the structure; C_f is an appropriate pressure or force coefficient; ρ is the air density; and U is the equivalent design wind speed for buffeting analysis.

The value of G_h is taken as 1.0 for the present calculation for reasons mentioned earlier. The other values assumed are as follows

K_z for the deck at $z = 16.5$ ft (5.03 m) = 0.385 (Table 6, ASCE 1990)
K_z for the arch at $z = 57.0$ ft (17.4 m) = 0.665 (Table 6, ASCE 1990)
I for a Category III structure $\quad$ = 1.11 (Table 5, ASCE 1990) at
$\qquad\qquad\qquad\qquad\qquad\qquad\quad$ hurricane oceanline

5

V for Houston, Texas $= 90$ mph or 40 m/s (Figure 1, ASCE 1990)

An expression for U can be written using Eqn. 3, as follows:

$$U = \sqrt{\frac{2q_z}{\rho}} \tag{5}$$

This equation and the above values yield $U = 62.0$ mph (27.6 m/s) for the deck and $U = 81.5$ mph (36.5 m/s) for the arch.

Equation 4 can be used to calculate the design static pressure (P) on the arch taking $U = 81.5$ mph (36.5 m/s), G_h as 1.40 corresponding to $z = 57$ ft (17.4 m) and Exposure B (ASCE 1990) and the coefficient of force $C_f = C_D = 2.90$ (normalized by arch depth $D = 38$ in. or 0.965 m). With these values $P = 69.0$ lb/ft^2 (3.3 kPa), which compares very well with the design pressure of 75 lb/ft^2 (3.6 kPa) used by TxDOT. However, for the deck where the mean wind speed U is only 62.0 mph (27.6 m/s) instead of 81.5 mph (36.5 m/s), and the drag coefficient C_D is only 1.64 (normalized with deck depth $D = 3.66$ ft or 1.12 m) instead of 2.90, the design wind pressure of 75 psf (3.6 kPa) used by TxDOT for static analysis is very much on the high side. For the deck, Eqn. 4 with U, G_h, and C_D values just mentioned gives the design pressure as 26.3 lb/ft^2 (1.3 kPa).

6. Analytical Studies: Numerical

6.1. Model Description

Analytical models of the tied arch bridge have now been formulated with one finite element computer code and work is underway to use a second code in a similar manner. The first code is called CDA/SPRINT. It is a version of MSC NASTRAN that has been scaled down for a desk-top computer. It is marketed by the CDA Group, 6019 S. Loop E, Houston, Texas 77033. This program has been used for all of the result presented herein. It is advantageous because of its ease in defining the structure and its graphical representation of the deflections and the modes of vibration of the structure. The second finite element program to be used soon is called ALGOR. It is a mini-computer version of SAP5 marketed by Algor, Inc., 150 Beta Drive, Pittsburgh, Pennsylvania, 15238-2932. It will be used in addition to CDA/SPRINT because CDA/SPRINT does not have the capability of finding the transient response of the bridge when different time histories of loading are imposed

at different points on the structure. Such loadings are necessary for non-coherent buffeting and for moving traffic loads on the bridge.

Figure 6.1 shows the first level of computer modeling of the complete bridge using CDA/SPRINT. This is the level used for dynamic analysis for the frequencies and modes of vibration and for some of the transient response results. The lower mode shapes will be depicted graphically with this model, although slightly more accurate frequencies were determined separately by considering symmetric and anti-symmetric modes of one-half the bridge from one end. A more detailed full model could not be utilized for dynamic analysis in CDA/SPRINT because of the code's limit of 225 degrees of freedom in determining the frequencies and mode shapes.

The elements in the computer model of Figure 6.1 consist of quadrilateral plate elements for the bridge deck and straight beam elements for the segments of the arches, the cables, the steel construction beams, and the concrete encasement of the construction beams. Similar elements will be used in the ALGOR model of the bridge. A more detailed model of the bridge is used for all of the static loading studies with CDA/SPRINT, since more than 225 degrees of freedom are allowed for static analysis. This more detailed model is shown in Figure 6.2. It has 2046 degrees of freedom. In all of the finite element computer solutions, only linear elastic response is considered.

Static and dynamic loading results have also been obtained below for an important stage of partial construction in the bridge's development, that is, with both arches erected and cross-braced to each other, but with the existing bridge removed and no new bridge deck units as yet attached. The steel for both arches will be erected and the arches will be braced to each other in one weekend's operation. After this the two arches should be almost as well supported as in the final condition. However, the long construction beams for the bridge will be vulnerable to the wind after the existing bridge is demolished and before the new bridge deck is installed so as to stiffen the steel construction beams. Temporary horizontal bracing will be required to stabilize the construction beams at this stage, which is likely to last at least a week, and perhaps several weeks. The time lag between demolition of the existing bridge and attachment of the new slab units will depend on whether consecutive weekends can be scheduled for each effort. Each effort will interrupt the

7

high-volume traffic of the freeway below and therefore can only be carried out on a weekend.

The bracing system assumed in this study is shown in Figure 6.3. It consists of horizontal struts straight across between the construction beams at the first hanger points from each end and then at alternating hanger points in the center portions, with diagonal tension counters in the horizontal plane between all of these points. The members used for the struts during this stage were chosen by TTU as 12" x 12" x 3/8" (305 mm x 305 mm x 9.5 mm) tubular members so as to limit the L/r ratio of the struts to 120, i.e. as "main members" in the steel codes. These choices were made before knowledge was gained concerning the struts designed by TxDOT, which were W12x65 wideflange sections, which have an L/r ratio of 179. This ratio is satisfactory if the members are considered to be "secondary members" because of the temporary nature of their function. The cables chosen for the diagonal tension counters were single cables of the same size as the hangers, that is, 1 5/8-inch (41.3 mm) bridge strand. TxDOT will use an alternate cable, a 2-inch (50.8 mm) diameter wire rope that is approximately equivalent to this bridge strand, for the hangers and for these counters, depending on the availability of the bridge strand.

6.2. Comparison to TxDOT Results

Computer results have been sent to Texas Tech from TxDOT in Houston for a few vertical loading cases and static behavior. These results were requested for checking Texas Tech's computer models. The two cases with results that can used are:

1) full dead load plus prestress (TxDOT 2D load case 40 and 3D load case 17); and
2) loading by trucks in three adjacent lanes at midspan plus sidewalk live loading, but without the dead loads or prestessing effects (TxDOT 2D total load case 50 minus case 40, and 3D load case 6).

Table 6.1 shows deflection comparisons for the two TxDOT loading cases. The Texas Tech results are with the detailed model of Figure 6.2, including 6 degrees of freedom per node. The point at which TxDOT deflections are given is on the construction beam at midspan on the more heavily load side. This point corresponds to point B in Figure 6.1. Table 6.1 also gives static loading results for the following points on the Texas Tech model: point A (the top of the arch), point C (the center

8

of the bridge at midspan), and point D (the edge of the deck at midspan).

Figure 6.4 illustrates the deflections in Table 6.1 as determined by Texas Tech for the first case, that of dead load plus prestress. Actually, the deck has been post-tensioned but is not composite with the steel superstructure at this stage of the construction process. The weight of the deck and the effect of the post-tensioning in the steel construction beam are included, but the steel superstructure (arches, hangers, and steel construction beams) must resist these forces. For this computation, the deck was removed and replaced with its weight, so the deck deflections in Figure 6.4 are shown for qualitative purposes only. The deflections of point A on the arch and point B on the construction beam are the ones of interest.

It may be seen from Table 6.1 that for both loading cases the Texas Tech model gives smaller deflections than the TxDOT results for the point of comparison, point B. The percentage difference is 17 % for the case of dead load plus prestress and 21 % for the sidewalk and truck loading. These differences are not of great concern in terms of the accuracy and consistency of the two models, but should be borne in mind in interpreting the remaining information in this report. Although the deflections differ by about 20 percent, the member forces differ between the two models only by approximately 10 percent and the support reactions by approximately 2 percent.

6.3. Static Responses

Three types of static responses are considered in this report. They are deflections and stresses due to vertical loads, horizontal design wind (75 psf or 3.6 kPa) loads, and buffeting wind loads of different types (drag, lift, and moment).

6.3.1. Vertical Loading – The two types of vertical loading of interest in this study are dead loads and live loads. Dead loads consist of the weights of all the bridge components. Vertical live loads consist of pedestrian, lane, and truck loads. The two loading cases shown in Table 6.1 cover calculations by two TxDOT models and by the Texas Tech model. The only live loads not included in this table are lane loads. Since such loads have been analyzed extensively by TxDOT, further cases have not been considered by Texas Tech. Such studies can still be carried out, however, if desired.

6.3.2. Design Wind Loading – Static wind loading represents the average or steady-state effect of the wind on the bridge. The design wind loading used by

TxDOT is 75 psf on all vertical surfaces parallel to the road. In this section static responses of the partially completed bridge and the completed bridge to TxDOT's 75 psf (3.6 kPa) loads are presented. They can then be compared to the static responses to the expected buffeting winds presented in the next section.

Table 6.2 gives selected static deflection and stress results for 75 psf (3.6 kPa) wind pressures on all vertical surfaces, as used in the TxDOT design. Data are presented for the construction stage and for the final bridge condition as discussed earlier. The results were obtained using the most detailed meshes in the CDA/SPRINT computer code for the complete bridge (Figure 6.2) and a corresponding mesh size for the construction stage of Figure 6.3. In all cases six degrees of freedom per node were included. Corresponding results with 3 degrees of freedom per node were less accurate in certain key locations.

The results in Table 6.2 show that wind loading by itself produces stresses that are far below design levels. The stresses in the deck are especially low, as expected, indicating that design wind loading should not control the design of the deck. In the completed bridge, the stresses shown must be added to the stresses from vertical loading. Since the allowable stresses are usually increased by one-third for wind loading, the combination of wind and vertical loading should not control. The stress levels are also about the same for both of the stages of construction considered, indicating that the support systems chosen for the partially constructed stages are adequate.

The lateral deflections in Table 6.2 are somewhat larger for the construction stage since there is no deck to stiffen the structure. However, these deflections are not excessive. The cross-bracing chosen to temporarily stiffen the construction beams at this stage causes the peak lateral deflections of these beams to be less than the peak deflections of the arch. The static wind deflections of the construction stage for 75 psf (3.6 kPa) loading are shown in Figure 6.5.

It should be noted at this stage that the deflections of the complete bridge shown in Table 6.2, which were computed using six degrees of freedom at each node of the detailed model of Figure 6.2, are larger than would be computed with the restricted model of Figure 6.1, which will be utilized later for dynamic computations. For dynamic results, CDA/SPRINT requires fewer than 225 degrees of freedom in the

entire model. Accordingly, the model of Figure 6.1 not only has fewer nodes (77 versus 341 for the model of Figure 6.2), but is limited to 3 degrees of freedom per node. Overall, counting constraints, the number of degrees of freedom is 2,046 in the model of Figure 6.2, but only 225 in the model of Figure 6.1. The degrees of freedom per node that are eliminated in Figure 6.1 for wind (i.e., lateral) loading are translations in the vertical (z) direction and rotations about the longitudinal and lateral (x and y) axes.

6.3.3. Mean Wind Lateral Loading – Static wind results for a model of buffeting (or gusty) winds are now considered. The model is based on the ASCE 7-88 wind design code (ASCE 1990). The basic wind speed V is taken as 90 mph (40.2 m/s) for Houston. This wind speed is considered to be the 50-year return period fastest mile wind at 33 feet (10.1 m) as measured at weather stations (usually airports). To find the corresponding wind speed and pressure at a different height in a different terrain several adjustments must be made. The deck of the bridge is approximately at the natural ground elevation, but the critical direction is from the east or west, or perpendicular to the span, and for this direction the reference level should be taken as the level of the freeway to be conservative. If the terrain of the bridge is exposure B (suburban), the importance factor for the bridge is taken as 1.11 (for a site in the hurricane oceanline and a category III structure), and the height of the arch is taken as 57 feet (17.4 m) above the freeway (the very top), then the mean velocity at that height is 81.5 mph (36.4 m/s). Next, if the drag coefficient C_D of the arch elements is 2.9, and the gust response factor G_h for this terrain and height above ground is taken as 1.40, then the mean wind pressure on the arch is 69.0 psf (3.3 kPa). A drag coefficient of 2.9 is appropriate for the sharp-edged rectangular box sections of the windward arch (ref.). The leeward arch should have a C_D that is somewhat less (between 1.3 and 1.6) because of shielding.

The pressure of 69.0 psf (3.3 kPa) just computed for the arch is a valid number for a static design procedure, but it is not the mean pressure. The gust response factor of 1.40 included in the computation above must be omitted in determining the mean pressure. Accordingly, the mean along wind pressure is only 49.3 psf (2.4 kPa).

For the deck, with the same terrain exposure and importance factor and a height

of 16.5 feet (5.0 m) above the freeway, the mean wind speed corresponding to the basic wind speed V of 90 mph (40.2 m/s) is only 62.0 mph (27.6 m/s). The appropriate C_D value for the edge of the deck and the encased (not sharp-edged) construction beam, as estimated from past wind tunnel tests, is only 1.64, and the gust response factor at this height is 1.63. The design wind pressure on the deck, including the gust response factor, thus is only 26.3 psf (1.3 kPa), which is a much smaller pressure than the TxDOT value of 75 psf (3.6 kPa) considered earlier. Furthermore, the mean wind pressure on the deck, found by omitting G_h, is only 16.1 psf (0.8 kPa).

Static responses to the arch and deck mean wind pressures just developed, considering the entire arch to be loaded as heavily as the top, are given in Table 6.3. It may be noted that these mean or steady state deflections due to buffeting are about one-half as large as those due to the 75 psf (3.6 kPa) design loading of Table 6.2. Similarly, the stresses in the members considered are between one-third and two-thirds of the values for 75 psf (3.6 kPa) loading.

6.3.4. Static Lift and Moment – Gusty winds can develop lift or downward force and moment effects on the deck of the TxDOT bridge as well as lateral pressures. A model for these effects has been formulated using assumed properties of the deck section, pending the results of the wind tunnel tests. The following formulas are used:

$$L(\text{lb/ft}) = (\frac{1}{2}\rho U^2)BC_L \quad \text{for the lift force, L}$$

$$M(\text{ft} - \text{lb/ft}) = (\frac{1}{2}\rho U^2)B^2 C_M \quad \text{for the moment, M}$$

where ρ is the mass density of the air (0.002378 slugs/ft^3 or 1.23Kg/m^3), B is the width of the deck (60 ft or 18.3 m), and C_L and C_M are the lift and moment coefficients for the deck. The values assumed for C_L and C_M are 0.5 and 0.01, respectively, pending the wind tunnel results. If C_L for the given deck is measured in the wind tunnel as negative then a downward force need to be considered instead of a lift force. Using the mean wind speed for the buffeting model at the height of the deck, 62.0 mph = 90.95 ft/sec (27.6 m/s), the lift and moment forces per unit length along the deck are 590 lb/ft (8.6 kN/m) and 708 ft-lb/ft (3.1 kN.m/m), respectively. The static deflections that result from these forces are given in Table 6.4. It may be seen that these vertical deflections are only about one-tenth as great as the vertical deflections

12

due to the static loads of Table 6.1, and the associated stresses are equally small.

6.4. Dynamic Responses

6.4.1. Vibrational Frequencies and Mode Shapes – The vibrational frequencies and mode shapes of the completed bridge are extremely important in determining its dynamic response to wind loading. Furthermore, different types of modes come into play in different ways. For vortex shedding and aeroelastic instability of the bridge, which relate essentially to the behavior of the deck in the wind, the most important modes are the lowest vertical and torsional ones. The first few modes whether vertical, torsional or lateral are the most important ones for buffeting of the completed bridge. Buffeting primarily produces dynamic response of the arches, although lift, moment and drag on the deck should be included for a complete analysis. It should be emphasized that later results in which the vertical and horizontal vibrations are not separated (i.e, with 6 degrees of freedom included for each node) will render more accurate natural frequency and mode results and include modes that combine vertical, horizontal, and torsional displacements. These modes could not be modeled with the SPRINT program for this bridge.

For the partially constructed portion of the bridge, only the horizontal frequencies and modes are important for the dynamic wind response. At this stage there is no chance of vortex shedding or aeroelastic instability of the structure because there is no deck. Thus, the only dynamic wind effects are buffeting effects, which depend on the lateral frequencies and modes.

The vibration results presented below for the completed bridge are obtained with the 225 degree of freedom model of Figure 6.1. This model gives frequencies that are very close to those of the more detailed model of Figure 6.2 for vertical motion, but frequencies that are slightly high for lateral motion. The results for the construction stage are with the model of Figure 6.3.

The lowest 18 vertical frequencies of vibration of the completed bridges are presented in the upper part of Table 6.5. Also given are brief descriptions of the modes, that is, whether or not they are symmetric or anti-symmetric about midspan and whether or not they involve torsion of the deck. Computer plots of the lowest six modes of vertical vibration are shown in Figure 6.6. These plots give more detail than the simple descriptions in Table 6.5 and help in visualizing the possible types

13

of dynamic behavior that the bridge can undergo. Corresponding shapes of the horizontal modes are shown in Figure 6.7.

The results in the upper part of Table 6.5 show that the first three modes involving torsion of the deck have very close frequencies (between 6 and 7 Hz) and are the only ones involving torsion in the frequency range of importance in wind analysis (less than 10 Hz). In fact, even modes with frequencies above 5 Hz, as these torsional modes have, are not likely to be strongly excited by the wind. This principal can be seen by examining the typical wind power spectra of Figure 6.8, which shows both vertical and along-wind horizontal spectra assumed in the buffeting wind model. A key point is that all the spectra have very small values above 5 Hz compared to the peak values below one Hertz. In contrast to the torsional mode frequencies, the lowest three frequencies of the bridge in purely vertical vibration do lie in the range of importance for wind analysis. For aeroelastic instability they are not as critical as the lowest torsional mode, but they still have a bearing on the deck behavior.

It should be noted that the fundamental mode of vibration of the completed bridge in vertical motion is anti-symmetric rather than symmetric, as for a girder type bridge. This fact is expected to have particular implications for the bridge's dynamic response to moving traffic loads. With an anti-symmetric first mode, a truck at the quarter-span point, rather than at midspan, has the greatest tendency to excite the fundamental mode.

The frequencies and modes of vibration of the bridge in horizontal motion, as shown in the lower part of Table 6.5, involve lateral vibration of the arches with no appreciable motion of the deck except for the eighth mode. The deck does participate in the 8th lateral mode (not included in Figure 6.7), but its frequency of 11 Hz is well above the range of concern for wind excitation. In fact, only the first and possibly the second modes of lateral vibration are likely to be excited by the wind since the other frequencies are all above 9 Hz.

Similar data for the horizontal frequencies and modes of the partially completed bridge are given in Table 6.6 and Figure 6.9. The structure is quite flexible and the lowest three frequencies of vibration are all less than 5 Hz. This structure is essentially just a box skeleton that is supported at its four base points. The box vibrates either laterally (lower and upper portions moving in the same directions) or

14

in torsion (lower and upper portions moving in opposite directions). Only the first symmetric and anti-symmetric torsional modes are included in the first six modes.

6.4.2. Buffeting Response – The one type of dynamic wind behavior that can be analyzed prior to obtaining results from the wind tunnel studies is buffeting. Actually, the effects of lift and moment on the deck that go into a complete buffeting analysis should be determined from wind tunnel results, but representative lift and moment values can be used as a first step. In the following results, a fully correlated set of lateral dynamic wind forces is applied to each of the two stages of construction of the bridge being considered. In these analyses the time history of the force at each point on the bridge is the same but the force magnitude is smaller for the deck than for the arch according to the smaller height above ground (16.5 ft or 5.03 m), vertical dimension exposed to the wind (3.167 ft or 0.97 m) and drag coefficient (1.64). Later a similar buffeting analysis is planned with a non-correlated wind using the ALGOR program. In the lateral results below, viscous damping equivalent to 2 percent in all modes is assumed for lateral vibration. One percent damping in all modes is assumed for vertical (lift) and rotational (moment) vibration of the deck.

The buffeting response of the bridge can be analyzed in two parts - the steady-state part and the dynamic part. The steady-state part is simply a static analysis under the pressures generated by the average wind. Results for this part have been given already in Table 6.3 and are shown again in the first column on each side of Table 6.7. The remaining columns of data in Table 6.7 are for dynamic response.

The time history of the lateral wind loading considered is shown in Figure 6.10. It is a statistically generated record representing the force per unit length on the arch. The mean wind speed of 81.5 mph (36.4 m/s) has been subtracted out to make the record a zero-mean process. It is a 90-second (1.5 minute) record of wind with a turbulence intensity factor of 0.40. This is a very high turbulence intensity, so the dynamic response of the structure is expected to be conservative, that is, larger than is likely to actually occur. A high turbulence intensity is used not only to give conservative results but to account for the fact that deck of the bridge is basically at ground level, where turbulence is large, even though the space below the bridge allows for the wind to have a high velocity at this level. The pressure time history has been generated to incorporate the wind frequency characteristics depicted in the

15

along-wind spectrum for the arch of Figure 6.8. It is digitized at time intervals of 0.05 seconds.

Figure 6.11 gives the first five seconds of the response of the top of the arch of the completed bridge on the windward side (point A in Figure 6.1) when subjected to the wind time history of Figure 6.10. As can be seen, the peak instantaneous deflection of this brief record is -0.1376 inches (-3.50 mm). The important feature of this figure is that it shows that the top of the arch responds almost exclusively in the first mode of lateral vibration. This mode has a frequency of 2.95 cycles per second, and there are 15 cycles in the 5-second duration of the plot.

A complete time history of the response of the top of the arch for the 1.5 minutes of the artificial wind record is presented in Figure 6.12. One can see from this figure that the peak positive and negative displacements are 0.634 inches (16.1 mm) and -0.710 inches (-18.0 mm), respectively. The positive and negative peak values should be of the same order for a zero-mean input, but they are not identical and will both be included in the results to follow. The time histories will not be given each time.

For the buffeting wind acting on the construction stage and the completed stage, the peak dynamic deflections of the same key points and the maximum dynamic stresses in the same members as studied under static loading are summarized in Table 6.7. Also given are the totals of the static and peak positive values. The peak dynamic deflections of the points considered are about twice the mean wind deflections (column 1) for the completed bridge, and of the same order of magnitude as the mean wind deflections for the partially completed stage, except for point B, the midspan point on the construction beam. This point has a much larger dynamic than static deflection, but the construction stage will be quite temporary and the associated stresses are not excessive. It is also interesting to compare the total (static plus dynamic) deflections in Table 6.7 to the corresponding static deflections under the 75 psf (3.6 kPa) design wind load (Table 6.2). The total wind deflections are approximately 50% higher than the design wind deflections for the completed bridge and the two are very close to each other for the partially completed stage.

Concerning the maximum member stresses on the right in Table 6.7, the most important conclusion is that the stresses are all so small that they should not pose any kind of danger to the structure. The total static and dynamic wind stresses

16

of Table 6.7 are generally somewhat larger than the corresponding stresses under 75 psf (3.6 kPa) loading, ranging from 50% smaller to over 100% larger. Still, the high percentage differences occur only where the absolute stresses are small, and the results as a whole indicate a safe design under the effects of lateral buffeting.

Dynamic deflections of the deck under unsteady (buffeting) lift and moment forces are shown in time history form in Figures 6.13 and 6.14. Damping ratios of 1 percent are included here for comparison with analytic frequency domain results. The actual damping in the bridge is difficult to estimate. Highway bridge damping measurements could not be found in the literature, and no bridge quite like the one under design has been built, much less field tested. Welded steel structures are generally known to have low damping coefficients (less than 2 percent), and prestressed concrete members have less damping than ordinary reinforced concrete ones because cracks do not open and close at design levels. Values of 1 percent and 0.5 percent are considered at different points in this report to ensure that conservatively large estimates of maximum deflections are obtained. For vertical vibration, damping due to air resistance of the deck could make the actual damping coefficient larger than these values. In Figures 6.13 and 6.14 the peak vertical deflections of point B on the construction beam at midspan are found to be 1.12 inches (28.5 mm) for the dynamic lift case and 0.0304 inches (0.8 mm) for the dynamic moment case. The angular rotation associated with the moment deflection is 11.25 E-5 radians. These peak dynamic values compare to static deflections of 0.088 inches (2.2 mm) and 1.67 E-5 radians, respectively, from Table 6.4. Here the dynamic values are of the order of 10 times the static values. The peak moment deflections are still small, but the lift deflection of point B is of the order of one-half the dead load deflection of this point from Table 6.1.

7. Analytical Studies: Empirical

7.1. Flutter Instability

Flutter instability describes an exponentially growing response of the bridge deck where one or more modes participate at a particular critical wind velocity resulting in failure due to overstressing of the main structural system. Flutter instability of the TxDOT bridge is assessed in this interim report using a set of assumed flutter-derivative coefficients. The flutter derivatives are dimensionless coefficients which

17

are functions of reduced frequency $K = \omega B/U$, where U = mean wind speed, ω = frequency in rad/s, and B = deck width. The levels of aeroelastic damping and aeroelastic stiffness due to the wind-deck interaction depend on these coefficients, which are strictly functions of the shape of the cross section and hence, can be obtained only through wind-tunnel testing. Since the first few modes are uncoupled, there is a possibility of having the aeroelastic damping drive the deck to flutter instability, i.e, damping-driven flutter.

The damping-driven flutter criterion is as follows:

$$H_1^*(K)G(h_i, h_i) + H_2^*(K)G(\alpha_i, h_i) + A_1^*(K)G(h_i, \alpha_i) \;+\; A_2^*(K)G(\alpha_i, \alpha_i)$$
$$\geq \; \frac{4\zeta_i I_i}{\rho B^4}\frac{\omega_i}{\omega} \qquad (6)$$

where

$$\left(\frac{\omega_i}{\omega}\right)^2 = 1 + \frac{\rho B^4}{2I_i} \; [H_3^*G(\alpha_i, h_i) + A_3^*G(\alpha_i, \alpha_i)] \qquad (7)$$

and where $G(r_i, s_i) = \int_0^l r_i(x)s_i(x)dx$ are the modal integrals in which r_i, $s_i = h_i$ or α_i are the vertical and torsional displacement components of the ith mode shape, l is the length of the bridge, ω_i is the frequency (rad/s) of the ith mode of vibration, I_i is the generalized mass of the ith mode of vibration, H_j^* and A_j^*, $j = 1..3$ are the flutter derivatives, ζ_i is the mechanical damping ratio of the ith mode of vibration, B is the deck width, and ρ is the air density.

Flutter derivatives of bridge deck no. 4 in Figure 7.1, which is similar to the Tied Arch bridge cross section without the traffic signs, are assumed for the present calculation. Bridge deck number 4 in Figure 7.1 has a similar shape except that it is inverted, which can be anticipated not to affect the flutter derivatives. The natural frequencies and mode shapes are taken to be the same as those found by the finite-element analysis, which were discussed in section 6.4.1 of the report. The deck width B is 60 ft (18.3 m) as furnished by TxDOT.

It has been found using Eqns. 1 and 2 that among all the modes of vibration, mode number 5 (1st torsional mode) is the most vulnerable to flutter, but it yields a physically unrealizable wind speed for flutter to occur. In this calculation the values of the critical damping ratios ζ_i for all the modes have been uniformly assumed to be 0.5%, which is a conservative (low) estimate.

A set of flutter derivatives for the bridge cross section with the traffic signs fixed on one side of the section is not available in the literature, so the flutter analysis for this case can be done after the wind-tunnel tests. However, it is comforting to note the following. If the flutter derivatives of the worst H-type bridge section like the old Tacoma Narrows is assumed for the flutter analysis of the present bridge, then the critical flutter speed is calculated as 114 mph. This critical flutter speed is higher than the design wind speed.

A more realistic assessment of the vulnerability to flutter can be made only after the wind-tunnel tests have been completed and the actual flutter derivatives of the present bridge deck, with and without the traffic signs, have been identified.

7.2. Buffeting Response of the Deck

A frequency-domain method is used to calculate the buffeting response of the deck. Earlier, a time-domain method was used to predict the buffeting response of the deck and the arch at various construction stages.

Buffeting forces act on a bluff body like a bridge deck or arch because of fluctuations in the wind speed, i.e, wind turbulence. These forces are also influenced by turbulence induced by the bluff body itself. To account for the body-induced turbulence, an aerodynamic admittance function $(\chi(n))$ is assumed for each of the three forces, i.e, the lift, moment and drag forces. For the present analysis the Sears Function is assumed as the admittance function, which can be approximated as $1/(1 + 5K)$, where K is the reduced frequency (Jancauskas 1983).

The parameters which influence the buffeting forces on the present bridge deck or arch are assumed as follows:

ρ $\quad$ = air density = 0.002378 slugs/ft^3 (1.23 Kg/m^3)

B $\quad$ = deck width = 60.0 ft (18.3 m)

D $\quad$ = depth of arch = 38.0 in. (965.0 mm)

C_L $\quad$ = coefficient of lift for the deck = 0.5 (normalized by B)

C_M $\quad$ = coefficient of moment for the deck = 0.01 (normalized by B^2)

C_D $\quad$ = coefficient of drag for the deck = 0.1 (normalized by B)

$\bar{C}_L, \bar{C}_M$ = coefficients of lift and moment for the arch = 0.0

$\bar{C}_D$ $\quad$ = coefficient of drag for the arch = 2.9 (normalized by D)

C'_L $\quad$ = $dC_L/d\theta$ = derivative of the lift coefficient for the deck with

19

respect to the angle of attack θ of the wind = 6.28

C_M' $= dC_M/d\theta =$ derivative of the moment coefficient for the deck with respect to the angle of attack θ of the wind = 1.57

The above values are conservative estimates and will be verified through wind tunnel tests on the section model. The flutter derivatives influence the buffeting response by modifying the mechanical damping ratios and the natural frequencies. The set of flutter derivatives used for flutter instability analysis are also used for this calculation.

In the present analysis the mean vertical response $(\bar{h})$, mean rotational or torsional response $(\bar{\alpha})$, mean lateral or along-wind response $(\bar{p})$ of the deck and the mean lateral response of the arch are computed using the equivalent design wind speeds U calculated in section 5 of this report and appropriate force coefficients. The corresponding mean square responses are calculated, as follows, to estimate the maximum excursion from the mean value.

Spectra of along-wind and vertical-wind turbulence (Eqns. 1 and 2) are assumed and used to obtain the spectra of the buffeting response and finally the mean square values of the response. In the field it is known that the spatial correlation of turbulence in the wind reduces with an increase in distance between two points along the span. In this calculation, it is assumed that turbulence is fully correlated along the span. This assumption gives a conservatively high estimate of the response. Calculations are made with U varying from 20 mph (8.9 m/s) to 80 mph (35.8 m/s), for along-wind turbulence intensities I_u of 25% and 40%, and for mechanical damping values ζ_i of 0.5% and 1.0% in all modes. The first ten modes of vibration are used to calculate the total response. The standard deviations (σ_h) of the maximum vertical response (h) and the standard deviations (σ_α) of the maximum torsional response (α) are listed in Tables 7.1 and 7.2 for the different combinations of U, I_u, and ζ, and these responses are plotted in Figure 7.2.

In Tables 7.1 and 7.2, the maximum standard deviations of the deck displacements are $\sigma_h^{max} = 0.059$ ft (0.018 m) and $\sigma_\alpha^{max} = 0.00024$ radians. These values correspond to the lower damping ratio of $\zeta = 0.5\%$ and the higher turbulence intensity $I_u = 40\%$ at a design wind speed of $U = 60$ mph (26.8 m/s). Since the first ten modes of vibration (see Table 6.5) have no lateral component (drag component), the deck's lateral displacement $\sigma_p^{max} \approx 0$.

20

The probability that the response of the deck lies within 3.5 σ bounds of its mean is 0.9998, if the probability distribution function (PDF) is assumed to be a normal distribution. In the absence of knowledge of the PDF, usually the Chebyshev inequality is used, which states that the probability of occurrence of any variable X within $m_x - c\sigma_x$ and $m_x + c\sigma_x$ bounds is $1 - \frac{1}{c^2}$. If c is taken as 3.5, then the probability becomes 0.92. Let c be 5.0 to get a probability of 0.96.

Therefore, there is a 96 % probability for the response to be within the following bounds:

$$
\begin{aligned}
h_{max} &\leq \bar{h} + 5.0 \times \sigma_h^{max} \\
\alpha_{max} &\leq \bar{\alpha} + 5.0 \times \sigma_\alpha^{max} \\
p_{max} &\leq \bar{p} + 5.0 \times \sigma_p^{max}
\end{aligned}
\tag{8}
$$

where $\bar{h}$, $\bar{\alpha}$ and $\bar{p}$ are the mean vertical, torsional and lateral deflections, respectively, as given in Table 6.4.

If $\sigma_h^{max} = 0.059$ ft (0.018 m) and $\sigma_\alpha^{max} = 0.00024$ radians from Tables 7.1 and 7.2 corresponding to $\zeta = 0.5\%$, $I_u = 40\%$ and $U = 60$ mph (≈ 62 mph $= 27.6$ m/s, design speed for the deck) are taken, then Eqn. 8 gives h_{max} and α_{max} as 0.31 ft (0.09 m) and 0.0012 radians, respectively, where the maximum mean responses are taken from Table 6.4.

7.3. Vortex-Induced Response of the Deck

Vortices will be shed from the deck at certain frequencies (f_s) and at different wind speeds according to the Strouhal number defined in Appendix C (Eqn. 12). When the frequency of vortex shedding matches one of the natural frequencies of the deck, the vortices will excite that particular mode of vibration. Vibration at this wind speed is called "lock-in." The first two vertical modes of vibration are most susceptible because they have the lowest frequencies. The Strouhal number St of the deck is taken as 0.15.

The lock-in wind speeds at which the first two modes may get excited are $U = f_n D / St = 1.40 \times 3.67 / 0.15 = 34.3$ ft/s $= 23.4$ mph (10.5 m/s) for the first mode, and $U = 2.32 \times 3.67 / 0.15 = 56.8$ ft/s $= 38.7$ mph (17. 3 m/s) for the second mode, using the natural frequencies obtained from the finite-element study. The lock-in wind speed for the third mode is 56.4 mph (25.2 m/s). Since a persistent wind speed is

required for lock-in to occur, and 23.4 mph (10.5 m/s) winds commonly persist in the Houston area, the first mode is the most vulnerable for vortex shedding. However, persistent wind speeds of 38.7 mph (17.3 m/s) are not impossible to occur, so the excitation of second mode is also considered in this calculation.

The steady-state amplitude of vibration can be calculated using Eqns. 13 and 14 (Appendix C) if values of two parameters Y_1 and ϵ are known for the present deck. These parameters depend on the deck shape and mechanical damping ratio (ζ) and can be obtained experimentally from a wind-tunnel test. The Strouhal number (St) also needs to be determined by wind-tunnel tests, but it normally varies over a fairly small range (0.12-0.15) for bridge decks. In the absence of experimental values, the parameters Y_1, ϵ, and St need to be assumed. The range over which ϵ varies is 500 to 1000 and the range over which Y_1 varies is 10 to 250, based upon past bridge deck studies. Conservatives estimate of Y_1 are made for the present calculations. Y_1 is assumed as 120 or 240. A value of Y_1 less than 85 will not lead to any vortex-shedding excitation even if $St = 0.12$ and $\zeta = 0.5\%$ are assumed. Hence, higher values are assumed in the absence of experimental results.

Steady-state vortex-excited amplitudes of vibration are listed in Table 7.3 for two values of St and two values of ϵ for both first and second modes of vibration. Full correlation of the vortices over partial spans on either side of the center point are assumed for the first mode in this calculation because it is anti-symmetric. Full correlation of the vortices over the entire span of the bridge is assumed for the second mode because it is symmetric. These assumptions are shown in Figure 7.3; these are reasonable for the present purpose. The mode shapes used are from the finite-element study discussed earlier. It can be seen that the maximum amplitudes of 0.29 ft (0.09 m) in the first mode at the lock-in wind speed of 29.2 mph (13.1 m/s) and 0.30 ft (0.092 m) in the second mode at the lock-in wind speed of 48.4 mph (21.6 m/s) result for the same combination of parameters. The maximum amplitude in the first mode of vibration will occur at each quarter point of the span and the maximum amplitude in the second mode of vibration will occur at the center point of the bridge span. The standard deviation of a sinusoidal response of amplitude A is $A/\sqrt{2}$. Therefore, the standard deviation of the response in the first or the second mode is equal to 0.21 ft. This standard deviation should be added to the

mean vertical lift displacement to get the total excursion as in the buffeting analysis (Eqn. 8). The maximum excursion of the vertical response at the mid-span location corresponding to $U = 48.4$ mph (21.6 m/s) can be calculated using Eqn. 8 as 1.06 ft (0.32 m), where the mean response is interpolated from Table 6.4. It needs to be mentioned that the value of maximum excursion is an extreme value estimate based on certain assumed statistics and a higher confidence limit.

The above calculation gives an upper bound on the amplitude of vibration due to vortex shedding. Normally, the damping ratio for a concrete structure like the bridge deck is assumed less than 2 percent. An increase in the damping ratio will either decrease the calculated amplitude or completely eliminate the anticipated vibration.

7.4. Dynamic Response of Deck Hangers

There are nine sets of hangers on each side of the deck which transfer the load from the deck to the arch. Each set of hangers consists of two bridge strands which are separated by 12 inches (305 mm) center to center. Each bridge strand is made of multiple wires and has an outer diameter of 1 5/8 inches (41.3 mm). The properties of the bridge strand and the tensile loads carried by the hangers were furnished by TxDOT.

The susceptibility of each of these hangers to vortex-shedding excitation is examined in this section. The procedures for calculating the natural frequencies and mode shapes of the hangers, the lock-in wind speeds and the amplitudes of vibration are given in Appendix C. It is found that motion due to vortex-shedding will take place only if the critical damping ratio of the hanger is below 0.05%. A damping ratio of 0.02% is assumed for the present calculation which is a very conservative (low) number. Table 7.4 lists the calculated values of the natural frequencies (f_n), the lock-in wind speeds (U) and amplitudes of vibration (Y_{max}) at the mid-height location of the hangers.

In every case $Y_{max} = 0.12$ inch (3.05 mm) because the steady-state vibration amplitude due to vortex shedding is dependent upon three parameters, namely: mass per unit length, diameter, and the assumed damping ratio of the hangers which are taken to be the same for all the hangers. Fully-correlated vortex shedding over the entire span of each hanger is assumed to get the above amplitude of 0.12 inch (3.05

23

mm). If it is assumed that the vortices are correlated only over the middle third of the hanger, then the values of the amplitudes reduce marginally to 0.10 inch (2.54 mm).

It can be concluded from the above analysis that even with a very low assumed damping ratio, the maximum amplitude of vibration is only 0.12 inch (3.05 mm). Hence, the expected motion of the hanger, if it vibrates at all, will be imperceptible and should not be a potential problem.

A wind-tunnel test will be carried out to verify the amplitude of vibration as predicted by the theory.

8. Wind-Tunnel Section Model and Experimental Set-up

A section model of the prototype has been built with 1:60 geometric scale. This choice of geometric scale is based upon the dimensions of the prototype and practical considerations associated with building section models. Photographs showing the section model details are given in Figure 7.4. The material chosen is aluminum instead of wood because the depth of the section is small enough to make it too flimsy if it is made of wood. However, the aluminum block used has been hollowed out as much as possible to make the model lighter (Figure 7.5). Two aluminum channels are added to represent the bottom chords of the prototype. The top of the deck of the model is covered with a rubbery material to represent the pavement geometry, including the correct amount of cant. The length of the section model is chosen as 40 inches (1.02 m) to utilize most of the wind-tunnel width.

A considerable effort has been devoted to designing the railing of the section model so as to represent the prototype chain-link fence aerodynamically. The vertical columns of the chain-link fence are represented by vertical rods with geometrically scaled (1:60) lengths but with differently scaled diameters. The wire mesh and the C-301 rail of the chain link fence are represented by seven horizontal rods spaced along the vertical direction. In the design process, the anticipated drag and moment (scaled values) due to wind flow on the chain link fence of the prototype have been closely matched to the expected drag and moment on the fence of the section model.

The end plates are made of aluminum and are attached at the ends to ensure two-dimensionality of the wind flow. Necessary accessories are attached at the ends to give the model two degrees of freedom, namely vertical and rotational or torsional.

24

A pipe of diameter 0.4 inch (90.2 mm) has been added near the bottom chord on the windward side to represent the 24 inch (610 mm) diameter water pipe on the prototype bridge. The 8 inch (203 mm) diameter pipe is less critical than the 24 inch (610 mm) pipe, and hence it has not been modeled.

The gear ratio between the motor and the fan which generates wind flow in the wind tunnel has been changed to give lower values of mean wind speed as required in this study. With this change, the wind speeds can range between 1 ft/s (0.305 m/s) and 60 ft/s (10.3 m/s).

Photographs of the suspension system of the model are given in Figure 7.6. In order to study the flow near the leading edge of the deck, smoke is generated at this location and photographs are taken. Figure 7.7 shows the vortices being generated at the leading edge of the bottom chord on the windward side of the deck at $U = 2.0$ ft/s (0.61 m/s).

9. Conclusions

Natural frequency and mode calculations, as well as time domain analyses of the buffeting response of the completed bridge and of the bridge in a critical stage of partial construction, have been carried out using the finite element code SPRINT. These studies show that for the completed bridge the peak dynamic stress ranges due to buffeting from a turbulent lateral wind with a basic wind speed of 90 mph (40 m/s) would be less than 2 ksi (67 MPa). Although a detailed fatigue analysis has not been performed, stresses of this magnitude should not create fatigue problems in the completed bridge. For the stage of partial construction when the existing bridge has been removed but the new deck has not yet been installed, the corresponding buffeting stress ranges could be considerably larger (up to 12 ksi) in the temporary horizontal braces chosen. However, there still should be no fatigue problem because of the very short time when this stage of construction can be subjected to the wind. Time-domain response calculations corresponding to a turbulent wind for lift and moment forces on the deck of the completed bridge have also been completed, and they indicate even lower levels of stress. Dynamic stresses due to moving traffic loads have not yet been determined.

Flutter analysis of the completed bridge deck for the configuration without the traffic signs shows that it is aeroelastically stable i.e, not likely to flutter. The flutter

analysis was based on a set of assumed parameters. For the bridge configuration with the traffic signs, no set of parameters were available in the literature for flutter analysis. Therefore, only wind-tunnel tests can give a definitive answer. However, even if the parameters of the worst H-type bridge section (like the old Tacoma Narrows) is assumed for flutter analysis, then the critical flutter speed is calculated as 114 mph (50.7 m/s) which is higher than the basic wind speed of 90 mph (40 m/s) of the deck.

An analytical assessment of the buffeting response of the deck was done in the frequency domain for vertical and torsional response. The parameters influencing the buffeting response were varied to find the maximum excursion of the response. It is found that there is a 96 % probability that the maximum response lies within 0.31 ft (0.09 m) for vertical and 0.0012 radians for torsion. These responses correspond to the basic wind speed of the deck (90 mph or 40 m/s) and assumed values of critical damping ratio (0.5%) and wind turbulence intensity ($I_u = 40\%$). The lateral buffeting responses of the deck for the completed bridge and the arch for the partially-constructed bridge are found using time-domain analysis and are found to be insignificant – peak deflection = 0.001 ft or 0.3 mm for deck and 0.18 ft or 0.06 m for arch. The damping ratio for the lateral loading case was assumed as 2%.

The vortex-shedding excitation of the deck seems to be more critical than buffeting in the present case. The lock-in wind speeds for exciting the first and the second modes of the bridge could be as low as 29.2 mph (13.1 m/s) and 48.4 mph (21.6 m/s), respectively. There is a 96 % probability that the vertical vibration amplitude of the deck at mid-span lies within 1.06 ft (0.32 m). This vibration amplitude has been obtained with a set of assumed parameters including a very low critical damping ratio of 0.5%. If the actual damping ratio is higher than the assumed value for the completed bridge, then the vibration due to vortex shedding will decrease.

The dynamic response analysis of the hangers due to vortex shedding shows that the maximum amplitude of vibration is 0.12 in. (3.05 mm), irrespective of different lengths of the hangers. This amplitude of vibration is calculated with 0.02% damping ratio which is a very low value. If the actual damping ratio is higher than 0.05%, which is more likely to be true, then the vortex-shedding excitation will be inconsequential. If the hangers vibrate, they will do so at different wind

speeds ranging between 4.70 mph (2.10 m/s) and 9.60 mph (4.29 m/s), but the low amplitude of vibration of 0.12 in. (3.05 mm) will be imperceptible and should not be a potential problem.

All the dynamic analyses reported herein are based upon assumed sets of parameters from the literature. Every bridge deck is unique aerodynamically and even a slight change in the same bridge cross section like the addition of traffic signs could change the bridge's aerodynamic properties. At this stage, it could be said that the completed tied arch bridge does not seem to have a potential problem based upon the parametric analysis reported herein. The section model of the bridge is already built and the wind tunnel tests are being performed. A more definitive answer can be given after all the wind-tunnel tests are completed. The authors would also like to analyze a few more cases of partially-constructed bridge configurations and include them in the next report along with the wind-tunnel results and traffic-loading results.

10. REFERENCES

ASCE (1990), "Minimum Design Loads for Buildings and Other Structures, ASCE 7-88, American Society of Civil Engineers, New York, NY.

Goswami, I. (1991), *Vortex-Induced Response of Circular Cylinders*, Thesis submitted in conformity with the requirements for Doctor of Philosophy, Dept. of Civil Engg., The Johns Hopkins University, Baltimore, MD.

Jancauskas, E. D. (1983), *The Cross-wind Excitation of Bluff Structures and the Incident Turbulence Mechanisms*, Thesis submitted in conformity with the requirements for Doctor of Philosophy, Dept. of Mechanical Engg., Monash University, Clayton, Victoria, Australia.

Scanlan, R. H. (1978), "State-of-the-Art Methods for Calculating Flutter, Vortex Induced, and Buffeting Response of Bridge Structures." *Federal Highway Administration Report No. FHWA/RD 80/50*.

Simiu, E. and Scanlan, R. H. (1986), **Wind Effects on Structures**, Second Edition, Wiley-Interscience Publications, New York.

APPENDIX A (Tables)

Table 6.1 Comparison of Static Midspan Vertical Deflections with TxDOT Results

Loading Case	TxDOT Deflection		Deflection of TTU Pt.			
	2D	3D	A	B	C	D
Dead Load Plus	-2.951 in.	-2.886 in.	-1.646 in.	-2.375 in.	—	—
Prestress	-74.96 mm	-73.30 mm	-41.81 mm	-60.33 mm	—	—
Sidewalk Loading	-0.965 in.	-0.834 in.	-0.481 in.	-0.659 in.	-0.784 in.	-0.592 in.
Plus Three Trucks	-24.51 mm	-21.18 mm	-12.22 mm	-16.74 mm	-19.91 mm	-15.04 mm
at Midspan						

30

Table 6.2 Static Deflections and Stresses Due to Design Wind Loading (75 psf or 3.6 kPa) (See Figures 6.2 and 6.3 for point and member locations)

Construction Stage	Lateral Deflection			Member Stresses		
	Pt.	Deflection		Member	Max. Stress	
		in.	mm		ksi	MPa
1) Construction Stage (Figure 6.3)	A	1.931	49.05	1 (top of arch)	0.615	4.240
	B	1.279	32.49	2 (top arch cross brace)	1.087	7.495
	E	2.142	54.41	3 (center of constr. beam)	1.542	10.631
				4 (beam cross brace)	6.358	43.841
2) Completed Bridge (Figure 6.2)	A	0.718	18.24	1 (top of arch)	0.305	2.103
	B	0.009	0.23	2 (top arch cross brace)	0.756	5.213
	E	0.828	21.03			

Table 6.3 Static Deflections and Stresses Due to Mean Lateral Wind Loading
(See Figures 6.2 and 6.3 for point and member locations)

Construction Stage	Lateral Deflection			Member Stresses		
	Pt.	Deflection		Member	Max. Stress	
		in.	mm		ksi	MPa
1) Construction Stage (Figure 6.3)	A	0.988	25.09	1 (top of arch)	0.310	2.137
	B	0.337	8.56	2 (top arch cross brace)	0.787	5.426
	E	1.096	27.84	3 (center of constr. beam)	0.580	4.000
				4 (beam cross brace)	1.673	11.535
2) Completed Bridge (Figure 6.2)	A	0.399	10.14	1 (top of arch)	0.200	1.379
	B	0.003	0.08	2 (top arch cross brace)	0.420	2.896
	E	0.460	11.68			

Table 6.4 Static Deflections Due to Mean Wind Lift and Moment Loading

Mean Loading	Vertical Deflection of Point				Associated Deck Rotation (radians)
	A	B	C	D	
1) Lift	0.057 in.	0.088 in.	0.125 in.	0.070 in.	0.00
	1.448 mm	2.235 mm	3.175 mm	1.778 mm	
2) Moment	0.003 in.	0.004 in.	0.000 in.	0.006 in.	1.67 E-5
	0.076 mm	0.102 mm	0.000 mm	0.152 mm	

Table 6.5 Frequencies and Modes of Vibration of the Completed Bridge

Direction of Vibration	Mode No.	Frequency (Hz)	Description
Vertical and Torsional Vibration	1	1.39	1st Anti-symmetric
	2	2.32	1st Symmetric
	3	3.38	2nd Symmetric
	4	5.17	2nd Anti-symmetric
	5	6.08	3rd symmetric - 1st torsional
	6	6.12	3rd Anti-symmetric - 2nd torsional
	7	6.94	4th Symmetric - 3rd torsional
	8	7.49	5th Symmetric
	9	7.78	4th Anti-symmetric
	10	7.90	6th Symmetric
	11	8.50	5th Anti-symmetric
	12	8.59	7th Symmetric
	13	8.84	6th Anti-symmetric
	14	9.63	7th Anti-symmetric
	15	10.6	8th Anti-symmetric
	16	11.1	8th Symmetric
	17	11.6	9th Symmetric
	18	11.7	10th Symmetric
Lateral Vibration	1	2.95	1st Symmetric
	2	6.92	1st Anti-symmetric
	3	9.06	2nd Anti-symmetric
	4	9.12	2nd Symmetric
	5	10.4	3rd Anti-symmetric
	6	10.5	3rd Symmetric
	7	10.8	4th Symmetric
	8	11.0	5th Symmetric - 1st lateral of deck
	9	12.9	4th Anti-symmetric
	10	16.0	6th Symmetric

34

Table 6.6 Horizontal Frequencies and Modes of Vibration of
the Partially Constructed Bridge

Mode No.	Frequency (Hz)	Description
1	1.87	1st Lateral Symmetric
2	2.89	1st Torsional Symmetric
3	4.58	1st Lateral Anti-Symmetric
4	6.29	2nd Torsional Anti-Symmetric
5	8.10	2nd Lateral Symmetric
6	8.96	3rd Lateral Symmetric

Table 6.7 Peak Dynamic Deflections and Stresses Due to Lateral
Wind Loading (See Figures 6.2 to 6.4 for point and member locations)

Construction Stage	Lateral Deflections				
	Pt.	Steady State	Peak Dynamic		Total (SS+ Pos.)
			Pos.	Neg.	
1) Construction Stage (Figure 6.3)	A	0.988 in. 25.10 mm	0.903 in. 22.94 mm	-0.971 in. -24.66 mm	1.959 in. 49.76 mm
	B	0.337 in. 8.56 mm	1.431 in. 36.35 mm	-1.276 in. -32.41 mm	1.768 in. 44.91 mm
	E	1.096 in. 27.84 mm	0.986 in. 25.04 mm	-1.069 in. -27.15 mm	2.165 in. 54.99 mm
2) Completed Bridge (Figure 6.2)	A	0.399 in. 10.13 mm	0.635 in. 16.13 mm	-0.710 in. -18.03 mm	1.034 in. 26.26 mm
	B	0.003 in. 0.08 mm	0.007 in. 0.18 mm	-0.007 in. -0.18 mm	0.010 in. 0.25 mm
	E	0.460 in. 11.68 mm	0.743 in. 18.87 mm	-0.832 in. -21.13 mm	1.203 in. 30.56 mm
	Member Stresses				
	Member	Steady State	Peak Dynamic		Total (SS+ Pos.)
			Pos.	Neg.	
1) Construction Stage (Figure 6.3)	1 (top of arch)	0.310 ksi 21.37 MPa	0.660 ksi 4.55 MPa	-0.660 ksi -4.55 MPa	0.970 ksi 6.69 MPa
	2 (arch x-brace)	0.787 ksi 5.43 MPa	0.588 ksi 4.05 MPa	-0.588 ksi -4.05 MPa	1.375 ksi 9.48 MPa
	3 (constr. beam)	0.580 ksi 4.00 MPa	0.246 ksi 1.70 MPa	-0.222 ksi -1.53 MPa	0.826 ksi 5.70 MPa
	4 (beam x-brace)	1.673 ksi 11.54 MPa	6.782 ksi 46.76 MPa	-6.782 ksi -46.76 MPa	8.455 ksi 58.30 MPa
2) Completed Bridge (Figure 6.2)	1 (top of arch)	0.200 ksi 1.38 MPa	0.619 ksi 4.27 MPa	-0.561 ksi -3.87 MPa	0.819 ksi 5.65 MPa
	2 (arch x-brace)	0.420 ksi 2.90 MPa	0.470 ksi 3.24 MPa	-0.419 ksi -2.89 MPa	0.890 ksi 6.14 MPa

Table 7.1 Standard Deviation of the Vertical Buffeting Response of the Deck (σ_h)

U	$\zeta = 0.5\%$		$\zeta = 1.0\%$	
	$I_u = 25\%$	$I_u = 40\%$	$I_u = 25\%$	$I_u = 40\%$
20 mph 8.9 m/s	3.41E-3 ft 1.04 mm	5.46E-3 ft 1.66 mm	2.99E-3 ft 0.91 mm	4.79E-3 ft 1.46 mm
40 mph 17.9 m/s	1.42E-2 ft 4.33 mm	2.27E-2 ft 6.92 mm	1.23E-2 ft 3.75 mm	1.97E-2 ft 6.00 mm
60 mph 26.8 m/s	3.70E-2 ft 11.28 mm	5.92E-2 ft 18.04 mm	3.04E-2 ft 9.27 mm	4.86E-2 ft 14.81 mm
80 mph 35.8 m/s	6.84E-2 ft 20.90 mm	0.110 ft 33.53 mm	5.61E-2 ft 17.10 mm	8.97E-2 ft 27.34 mm

Table 7.2 Standard Deviation of the Torsional Buffeting Response of the Deck (σ_α radians)

U	$\zeta = 0.5\%$		$\zeta = 1.0\%$	
	$I_u = 25\%$	$I_u = 40\%$	$I_u = 25\%$	$I_u = 40\%$
20 mph 8.9 m/s	1.10E-5	1.76E-5	1.10E-5	1.76E-5
40 mph 17.9 m/s	3.19E-5	5.10E-5	3.19E-5	5.10E-5
60 mph 26.8 m/s	1.50E-4	2.40E-4	1.07E-4	1.71E-4
80 mph 35.8 m/s	1.93E-4	3.09E-4	1.73E-4	2.76E-4

Table 7.3 Vortex-Shedding Vertical
Deflection of the Deck

Mode	St	U	Y_1	ζ	$\epsilon = 500$	$\epsilon = 1000$
1	0.12	29.2 mph 13.1 m/s	120	0.5%	0.18 ft 54.9 mm	0.13 ft 39.6 mm
1	0.12	29.2 mph 13.1 m/s	240	0.5%	0.29 ft 88.4 mm	0.20 ft 61.0 mm
1	0.15	23.4 mph 10.5 m/s	120	0.5%	0.08 ft 24.4 mm	0.06 ft 18.3 mm
2	0.12	48.4 mph 21.6 m/s	120	0.5%	0.20 ft 61.0 mm	0.14 ft 42.7 mm
2	0.12	48.4 mph 21.6 m/s	240	0.5%	0.30 ft 91.4 mm	0.21 ft 64.0 mm
2	0.15	38.7 mph 17.3 m/s	120	0.5%	0.13 ft 39.6 mm	0.09 ft 27.4 mm

38

Table 7.4 Dynamic Response of Hangers

Hanger No.	Length	Tension	f_n (Hz)	U	Y_{max}
1,9	16.25 ft 4.96 m	76.3 kips 339.4 kN	20.74	9.60 mph 4.29 m/s	0.12 in. 3.05 mm
2,8	23.75 ft 7.24 m	81.7 kips 363.4 kN	14.68	6.80 mph 3.04 m/s	0.12 in. 3.05 mm
3,7	30.00 ft 9.15 m	77.1 kips 343.0 kN	11.29	5.20 mph 2.32 m/s	0.12 in. 3.05 mm
4,6	31.25 ft 9.53 m	75.0 kips 333.6 kN	10.69	4.90 mph 2.19 m/s	0.12 in. 3.05 mm
5	32.50 ft 9.91 m	74.2 kips 330.1 kN	10.22	4.70 mph 2.10 m/s	0.12 in. 3.05 mm

APPENDIX B (Figures)
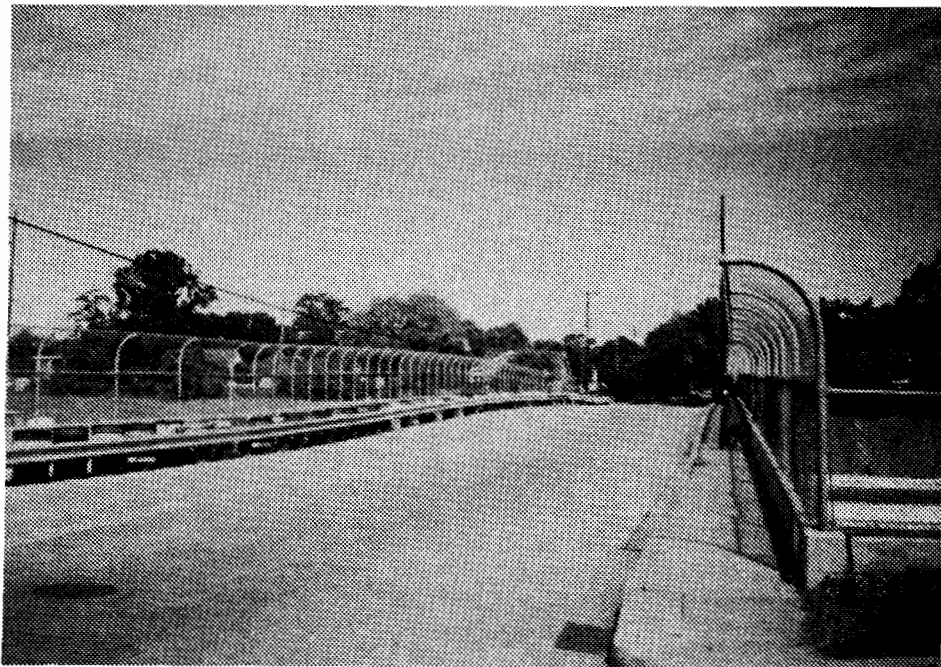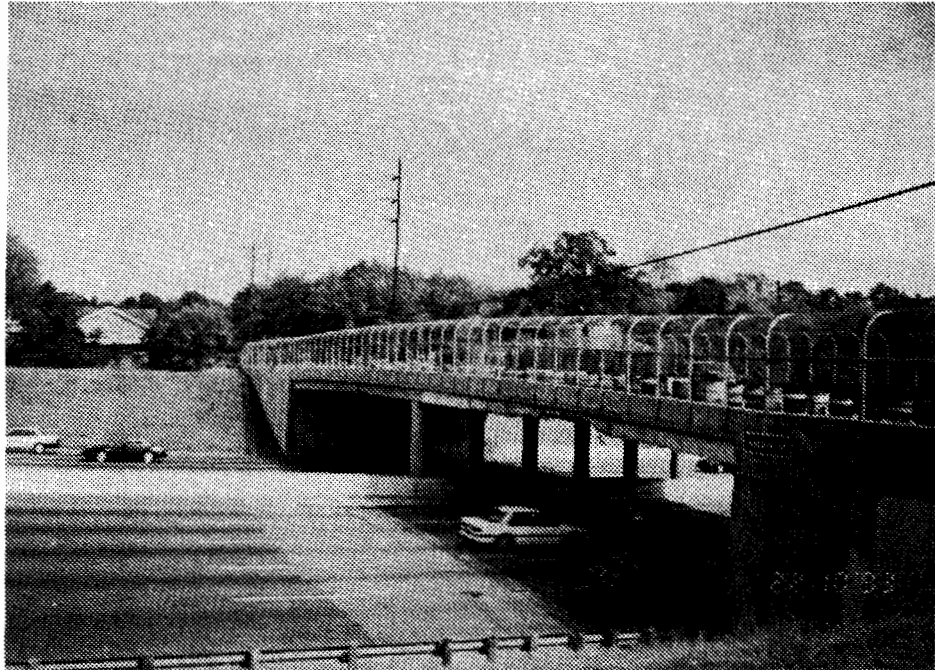
Figure 1.1 Photographs of the Existing Bridge

41
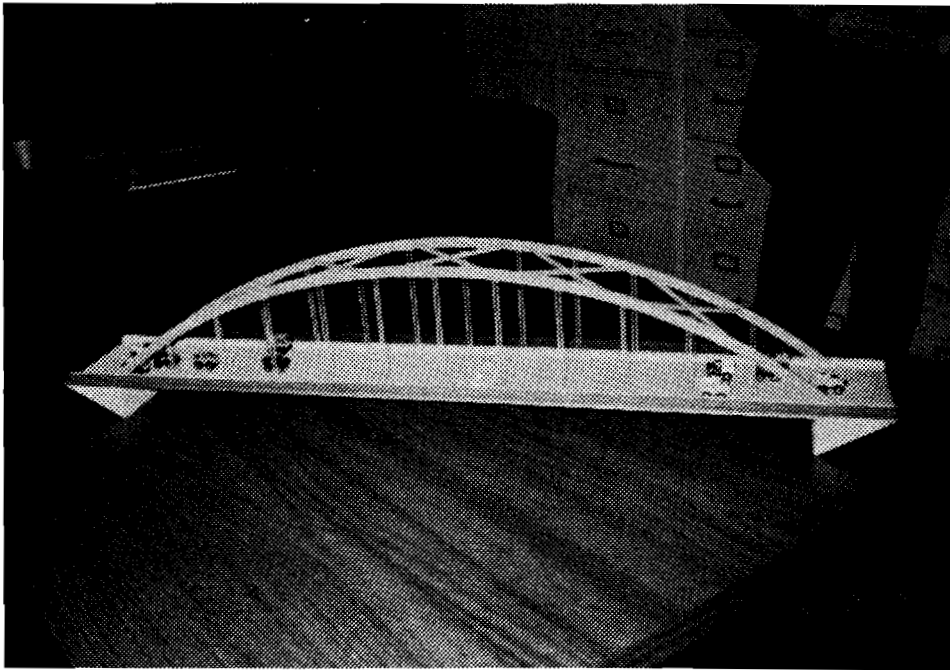
Figure 4.1 Model of a Typical Tied Arch Bridge (Houston Office, TxDOT)
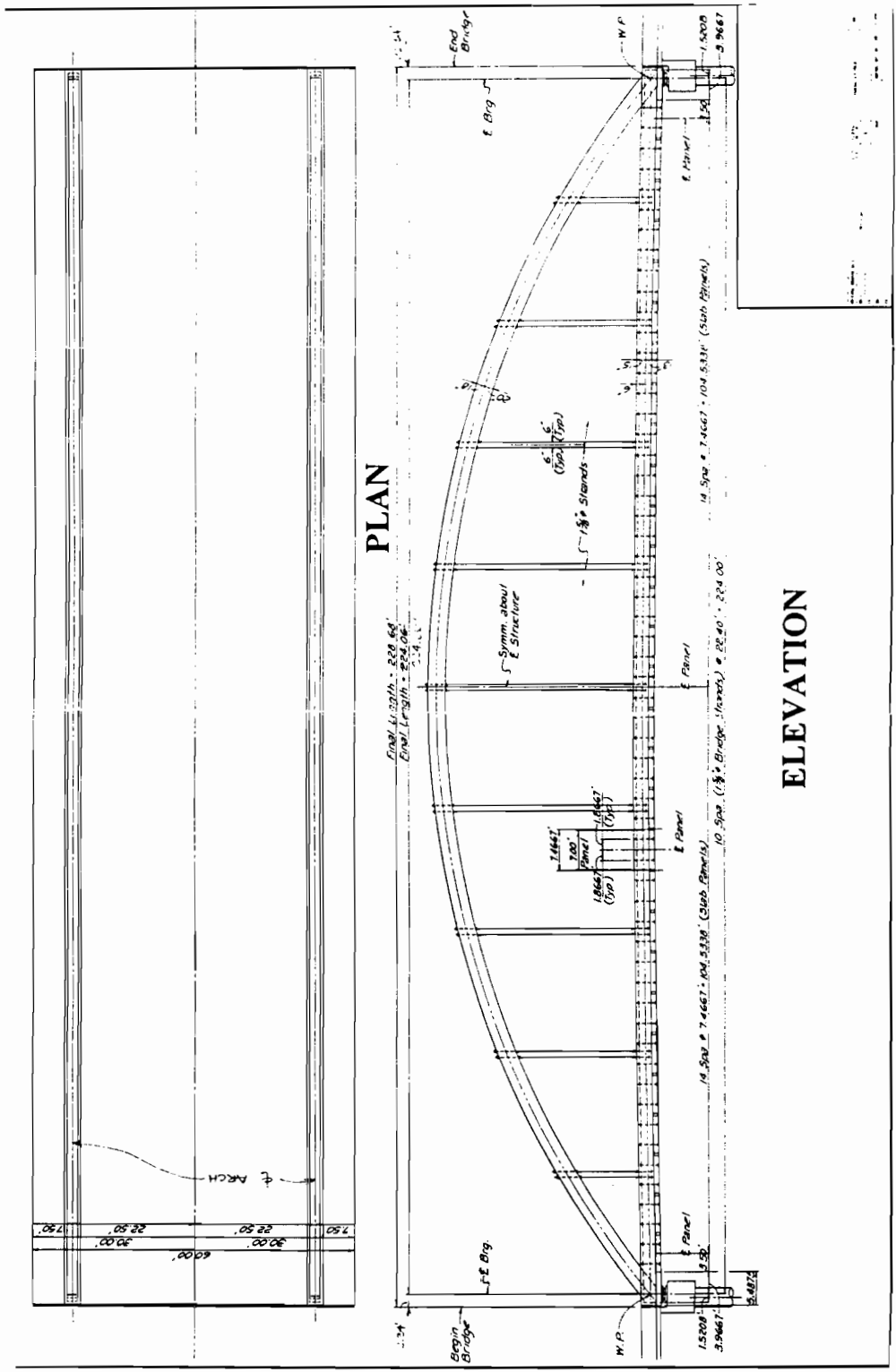
Figure 4.2 Plan and Elevation of a Typical Tied Arch Bridge
(Houston Office, TxDOT)

43
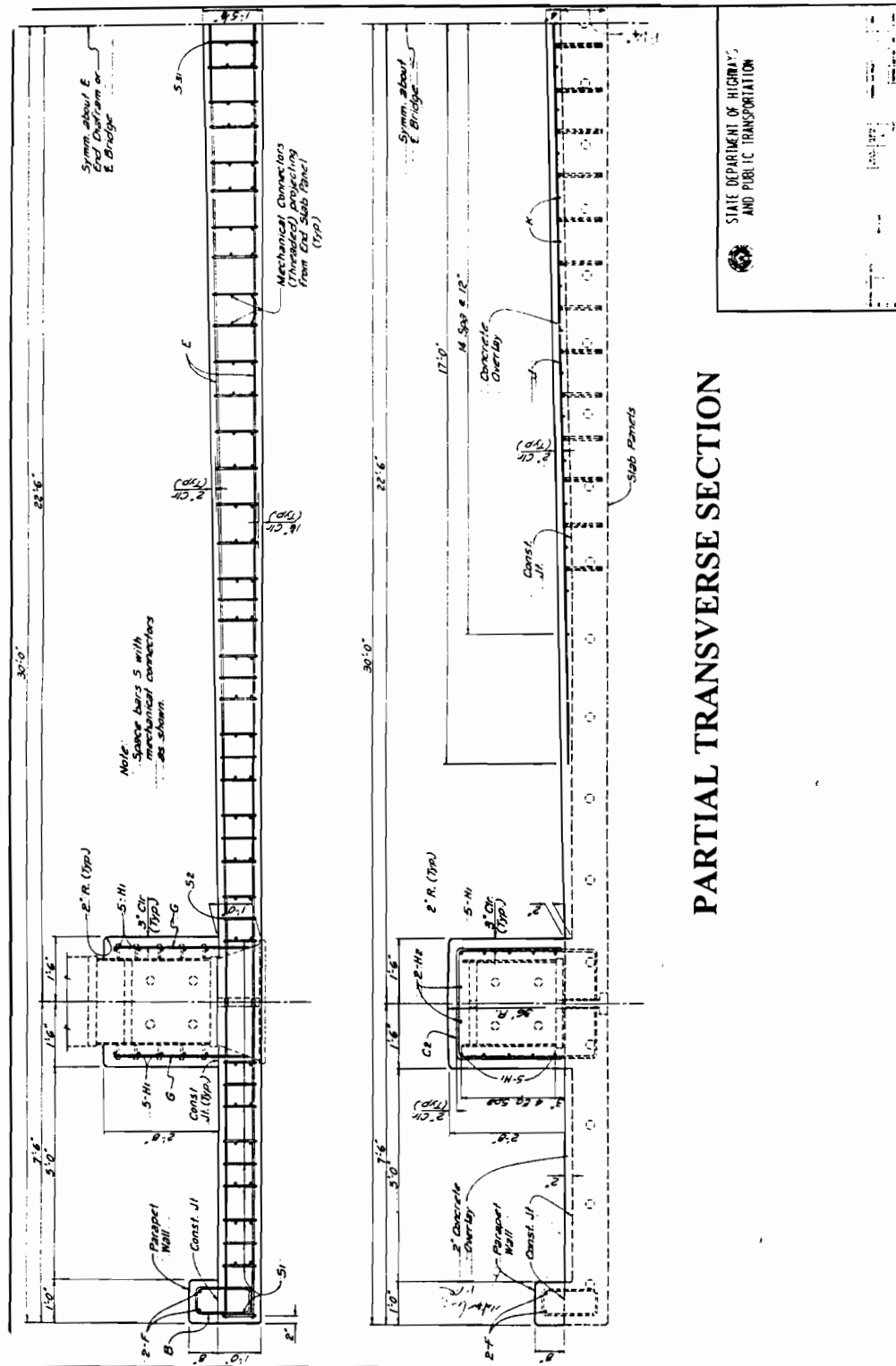
Figure 4.3 Cross-section of the Deck of a Typical Tied Arch Bridge
(Houston Office, TxDOT)

44
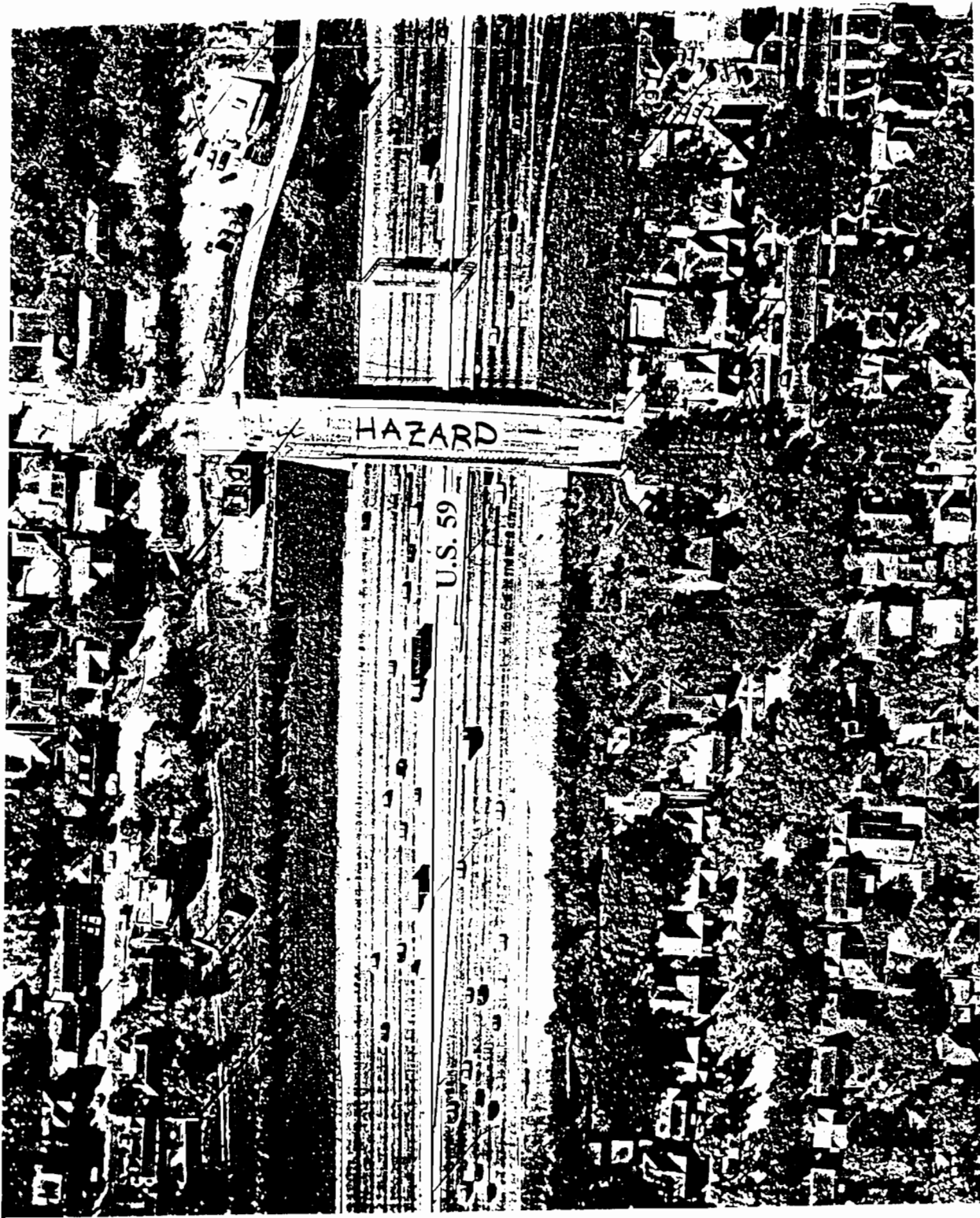
Figure 5.1 Aerial View Showing Location of the Existing Bridges on
U.S. 59 in Houston, TX
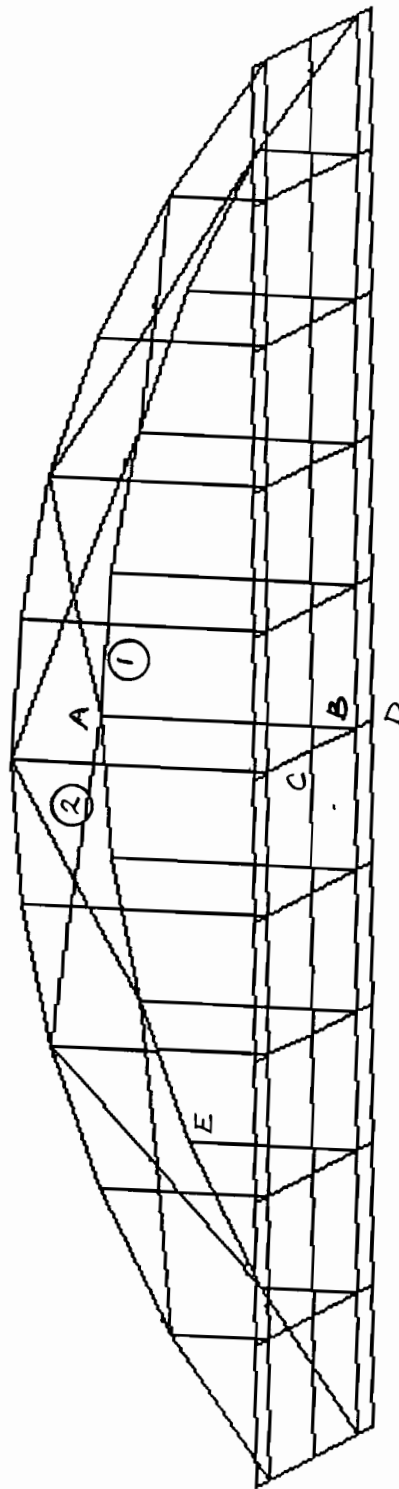
Figure 6.1   First Level Model of Complete Bridge (77 Nodes) Using SPRINT
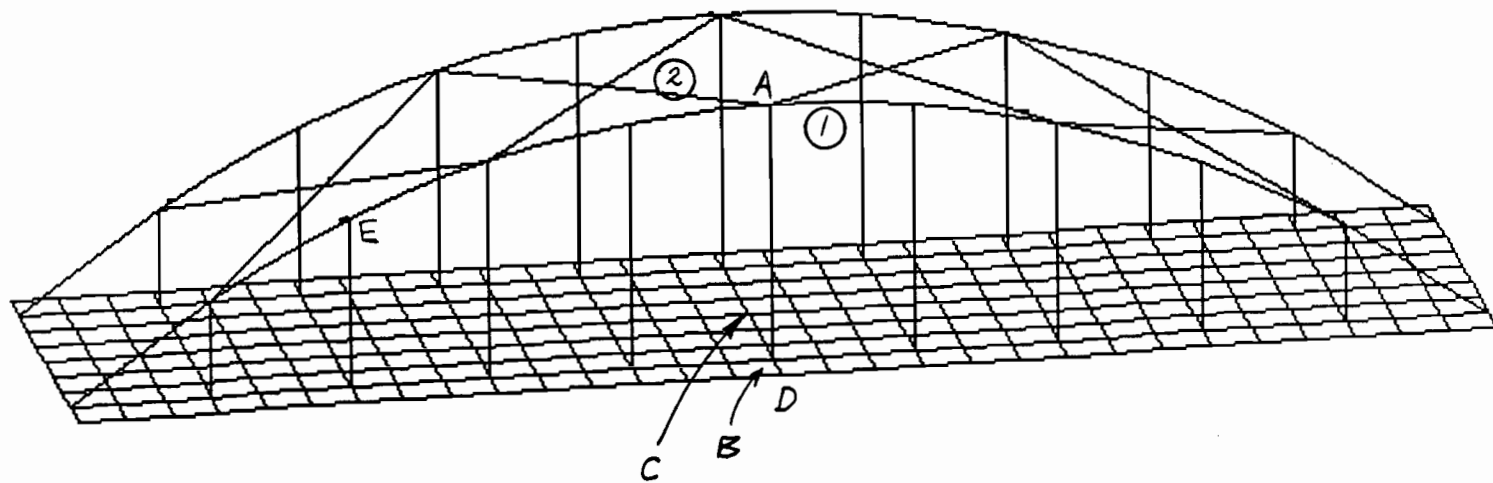
Figure 6.2   Second Level Model of Complete Bridge (341 Nodes) Using SPRINT
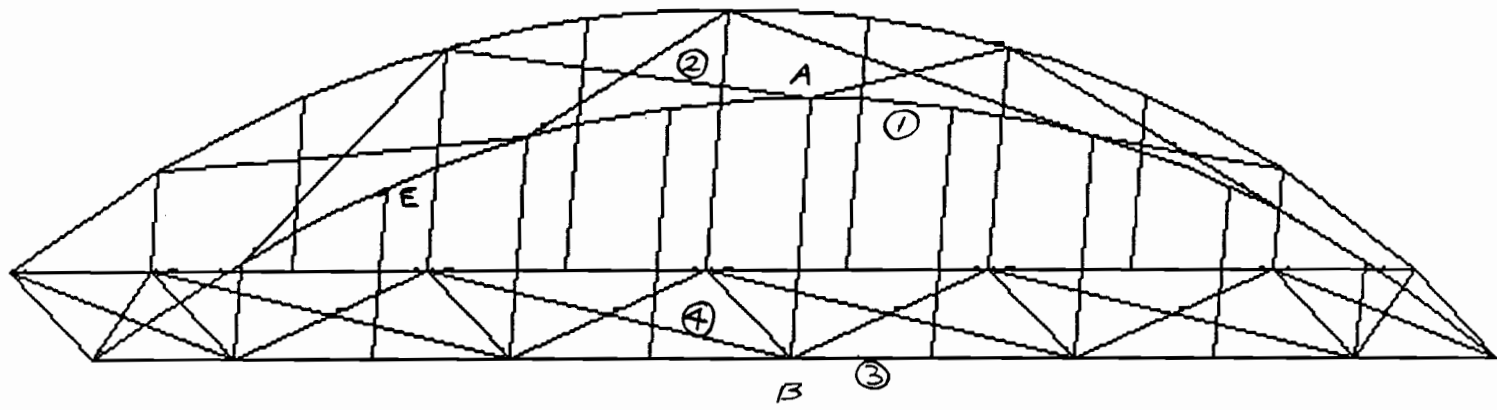
Figure 6.3   Second Level Model - Partial Construction Stage (124 Nodes) Using SPRINT
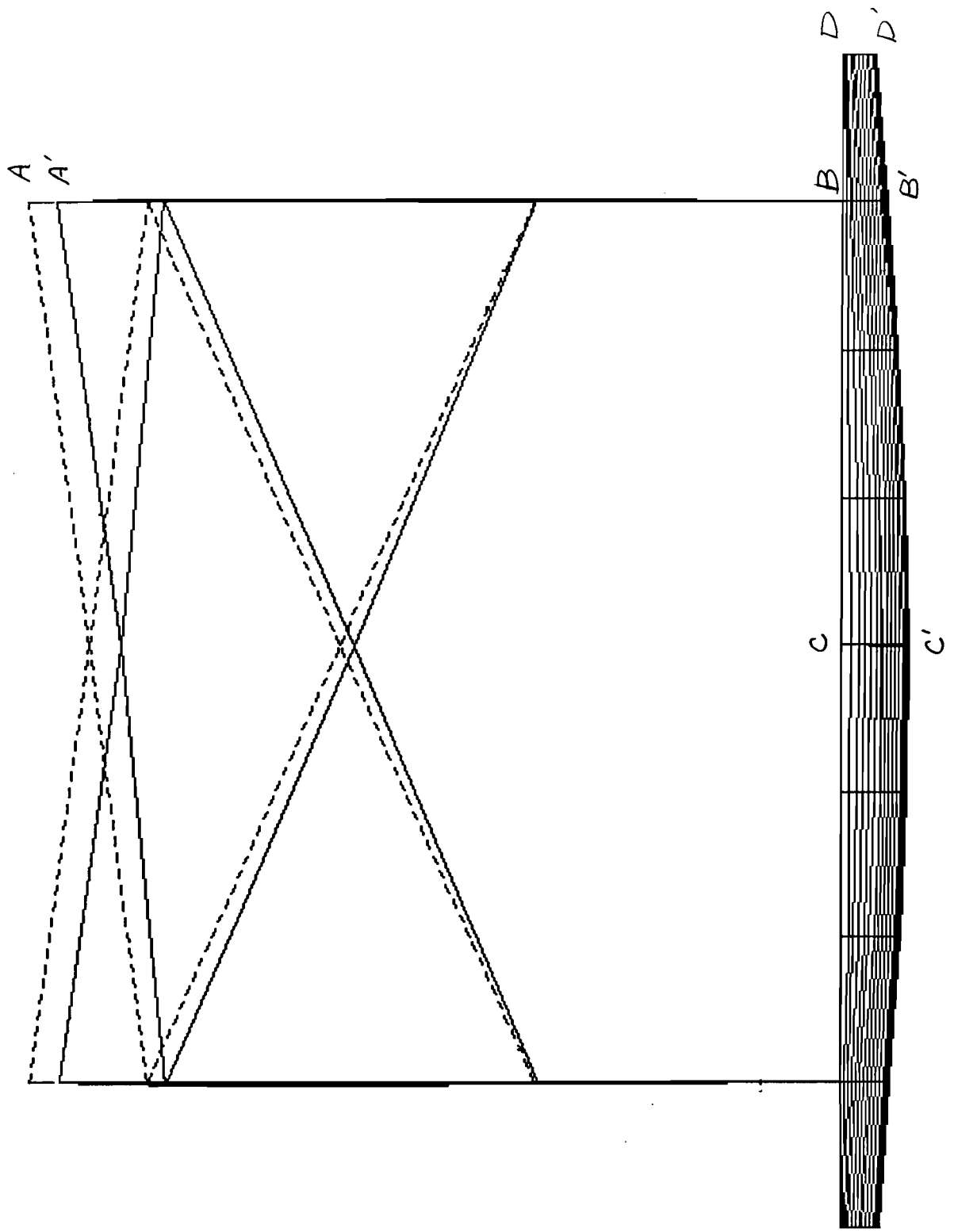
Figure 6.4   Deflections of Completed Bridge Under Dead Load Plus Prestress

49

$\delta_{max} = 2.15$ in. $\delta = 1.93$ in.
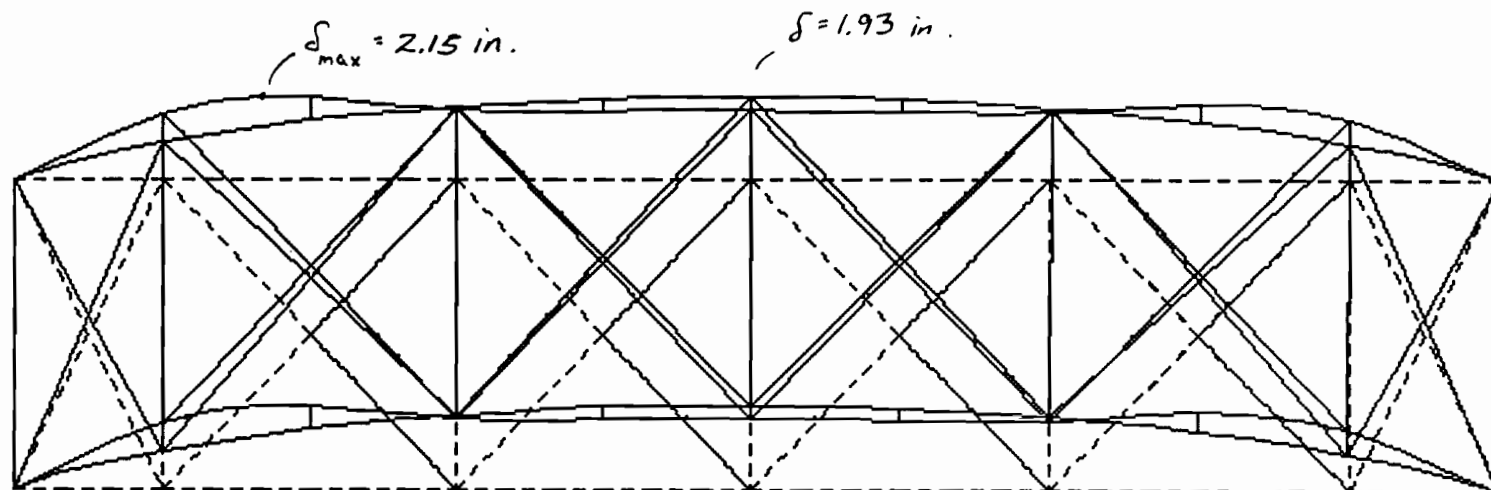
Figure 6.5   Static Wind Deflections Under 75 psf for the Partial Construction Stage
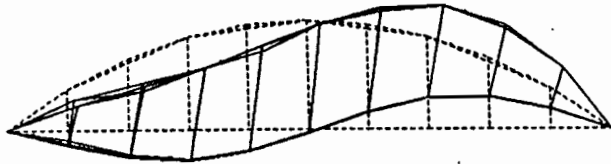
First Mode, f_1 = 1.39 Hz
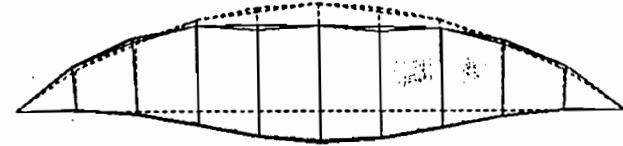
Second Mode, f_2 = 2.32 Hz
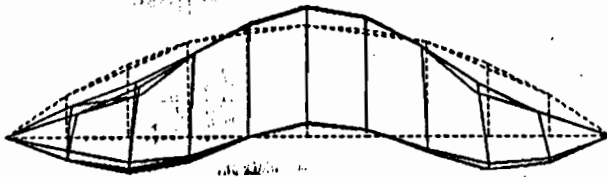
Third Mode, f_3 = 3.38 Hz
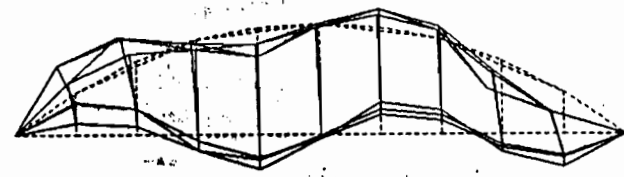
Fourth Mode, f_4 = 5.17 Hz
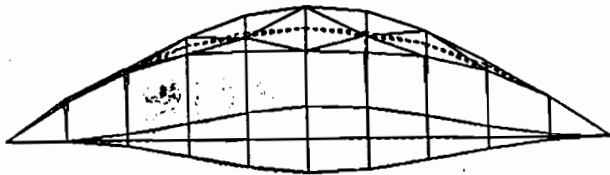
Fifth Mode, f_5 = 6.08 Hz
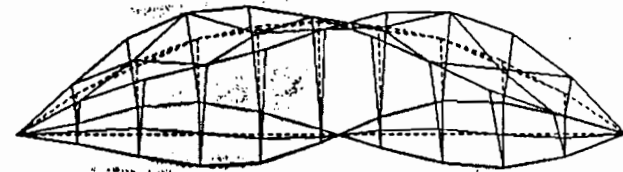
Sixth Mode, f_6 = 6.12 Hz

Figure 6.6   First Six Vertical Frequencies and Modes - Complete Bridge
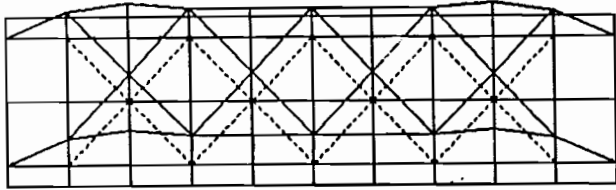
First Mode, f_1 = 2.95 Hz
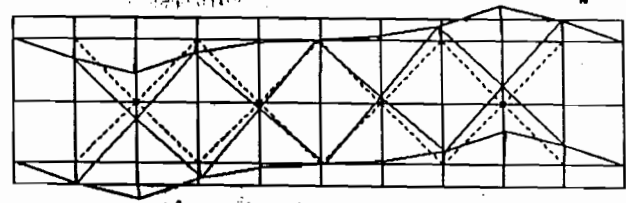
Second Mode, f_2 = 6.92 Hz
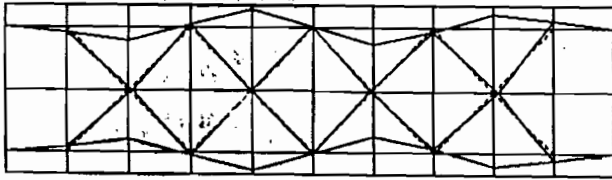
Third Mode, f_3 = 9.06 Hz
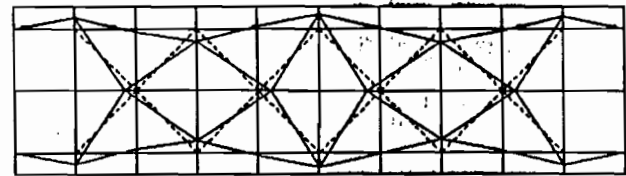
Fourth Mode, $f4$ = 9.12 Hz
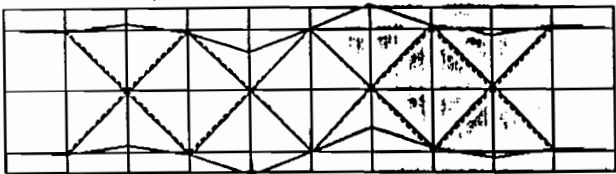
Fifth Mode, f_5 = 10.4 Hz
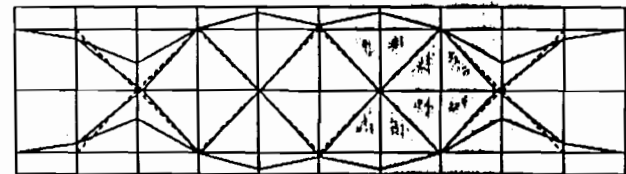
Sixth Mode, f_6 = 10.5 Hz
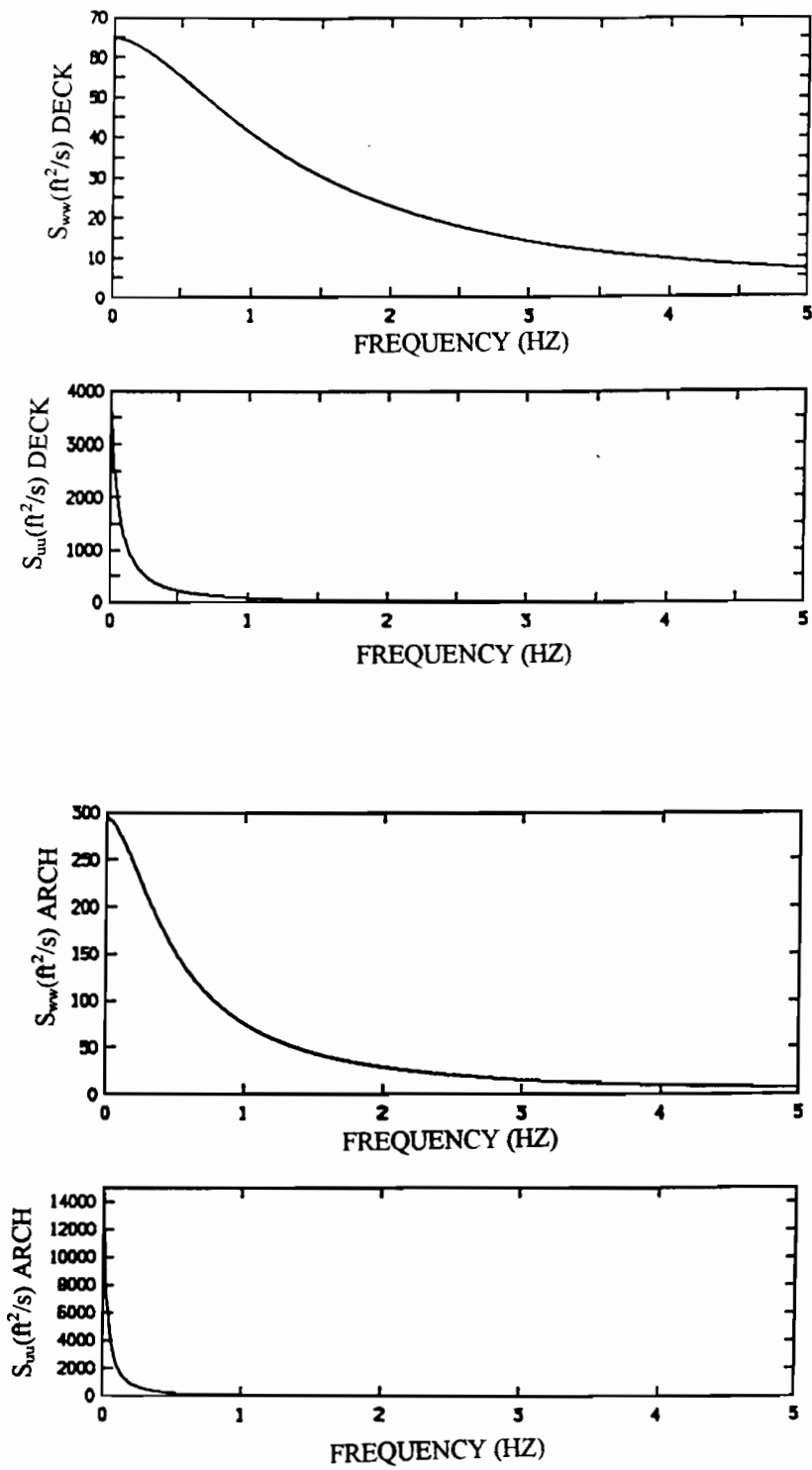
Figure 6.8   Assumed Along-Wind and Vertical Power Spectra for Arch and Deck
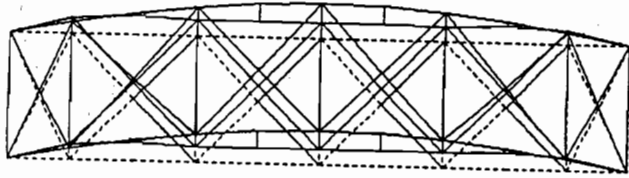
First Mode, f_1 = 1.87 Hz
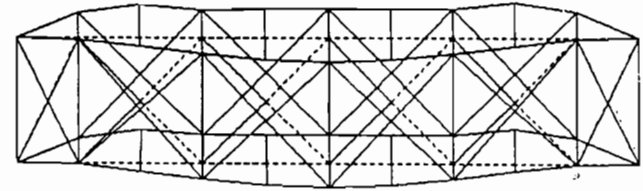
Second Mode, f_2 = 2.89 Hz
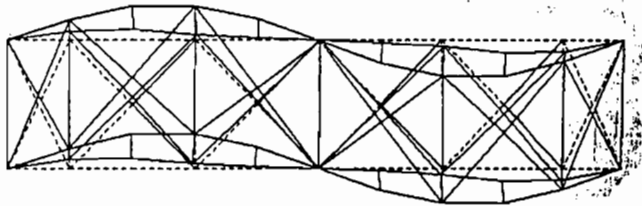
Third Mode, f_3 = 4.58 Hz
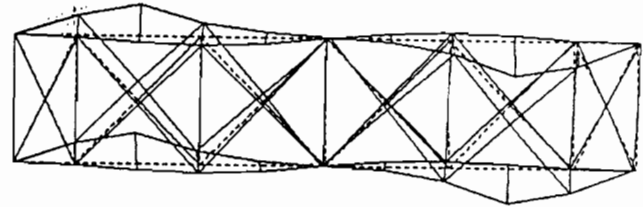
Fourth Mode, f_4 = 6.29 Hz
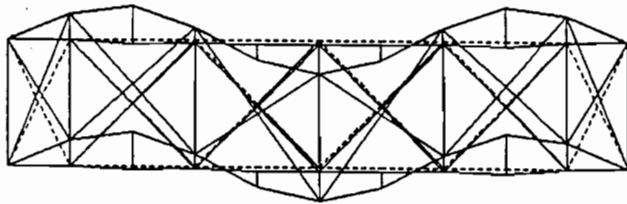
Fifth Mode, f_5 = 8.11 Hz
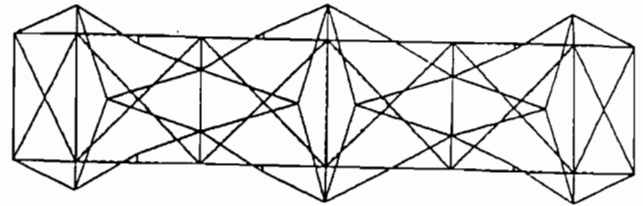
Sixth Mode, f_6 = 8.96 Hz
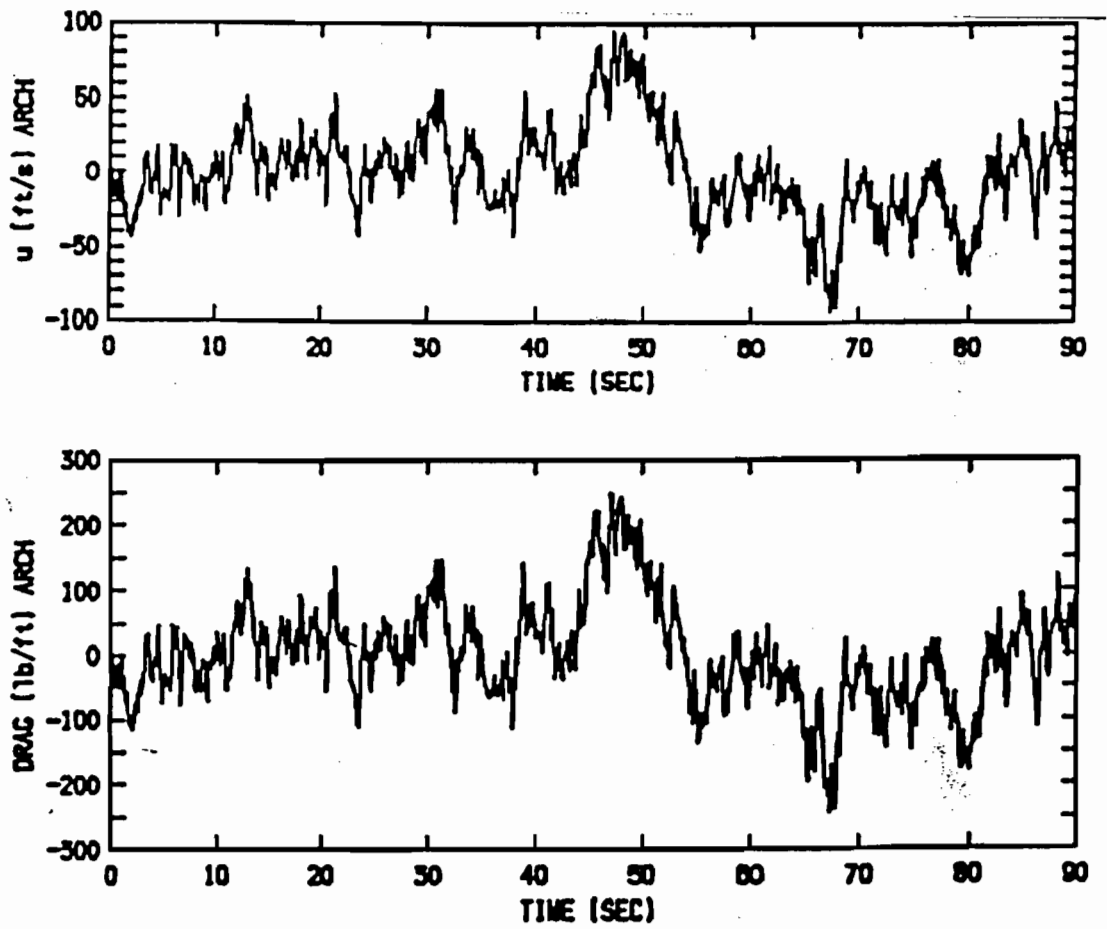
Figure 6.10   Time Histories of Wind Velocity and Wind Loading - Top of Arch

55
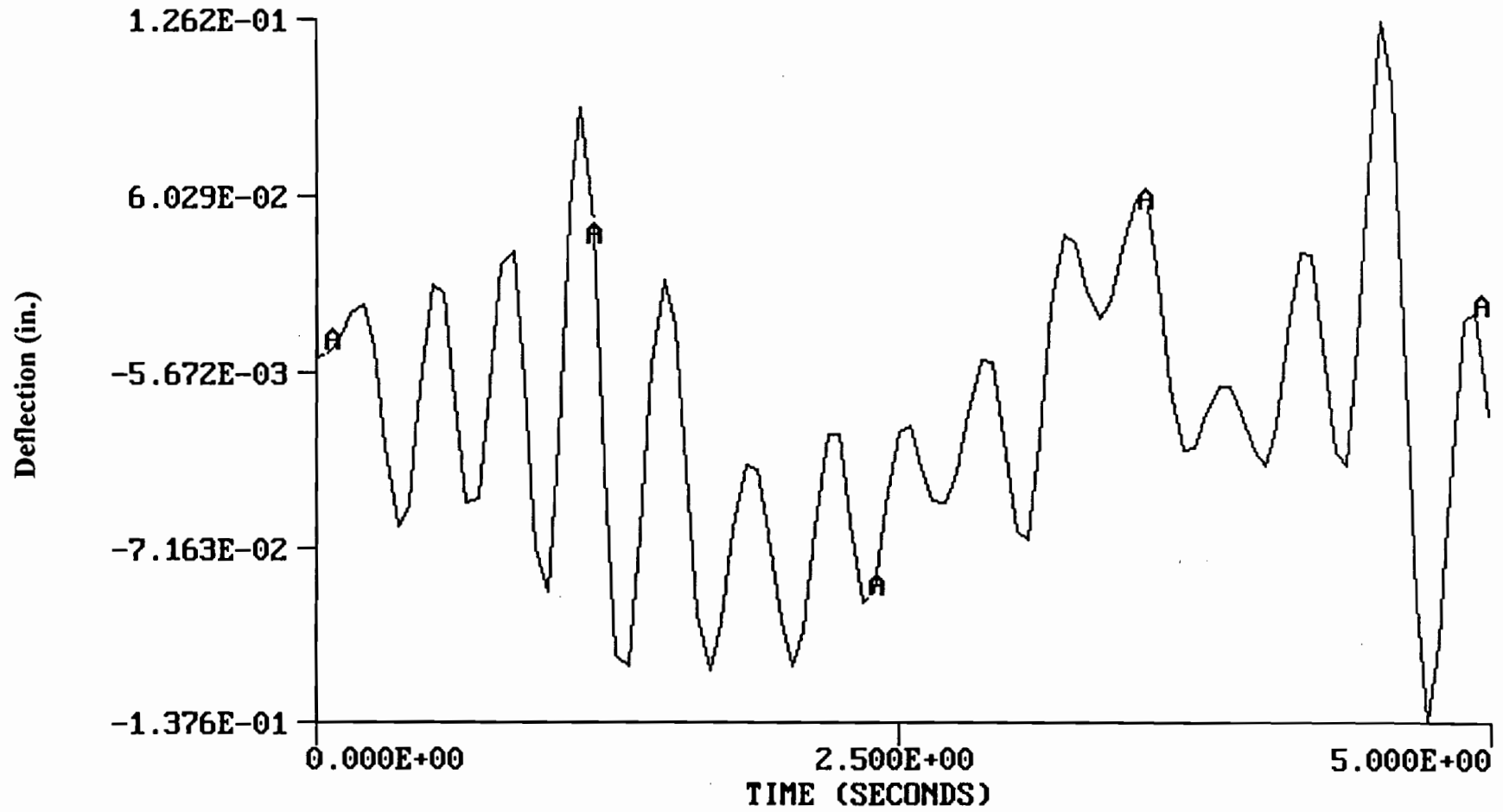
Figure 6.11 First Five Seconds, Dynamic Lateral Deflection - Top of Arch
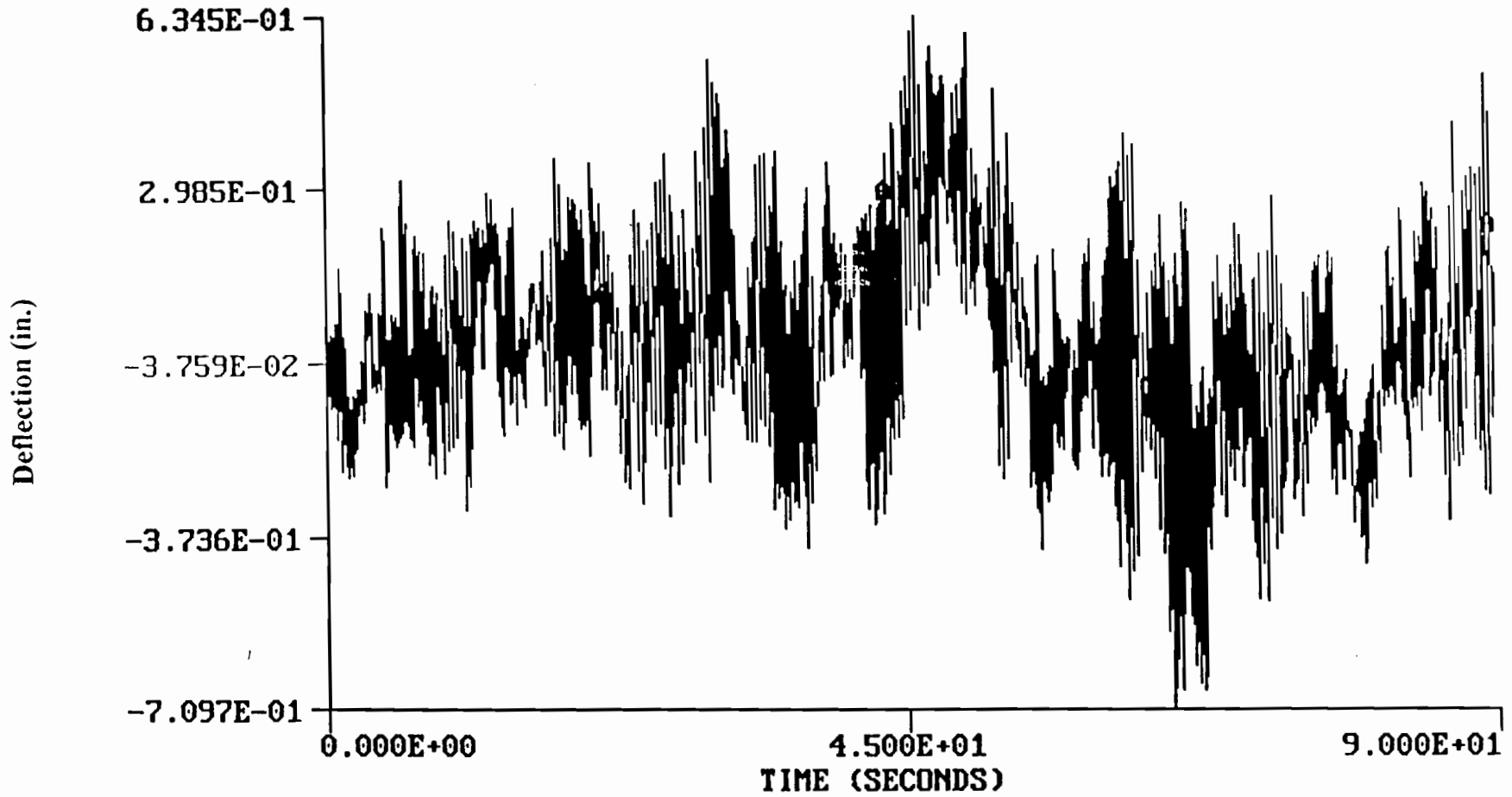
Figure 6.12   1.5-Minute Record, Dynamic Lateral Response - Top of Arch
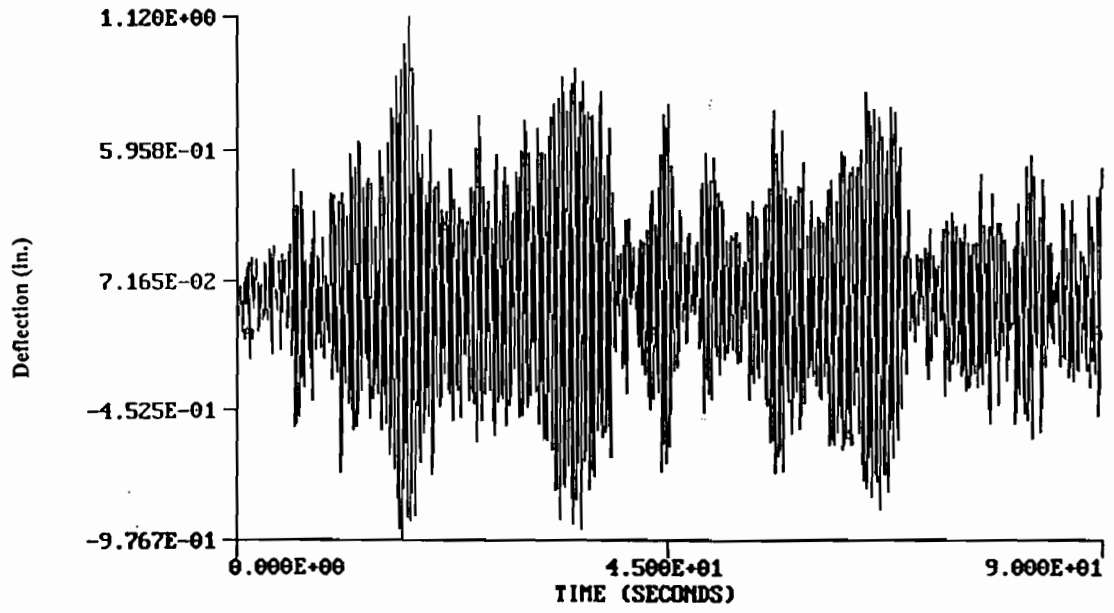
Figure 6.13   Dynamic Vertical Deflection of the Deck at Midspan Due to Lift
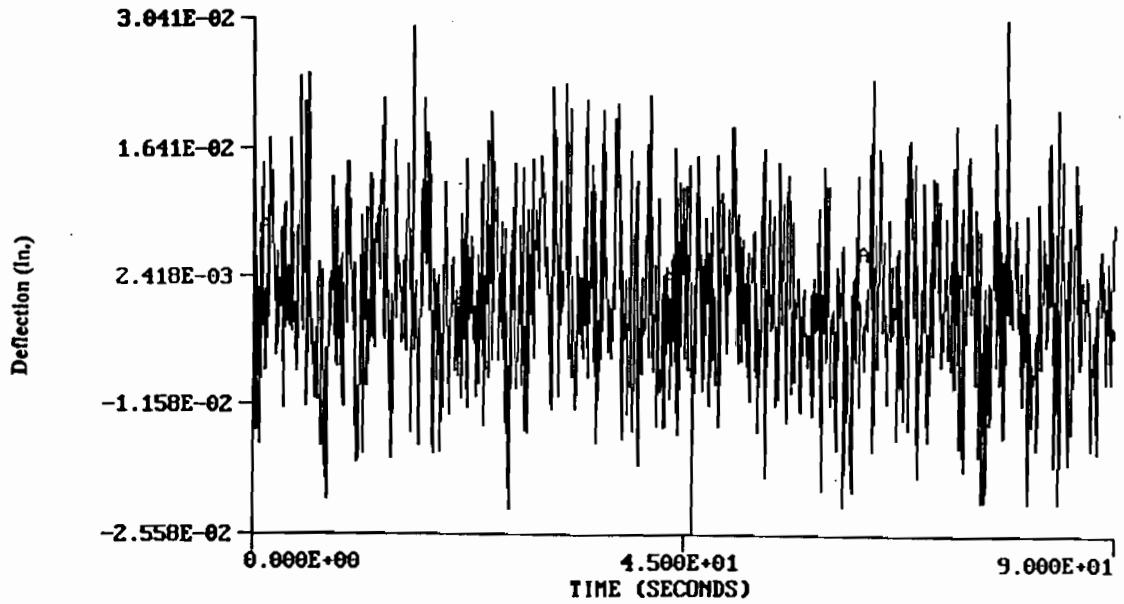
Figure 6.14   Dynamic Vertical Deflection of the Deck at Midspan Due to Moment
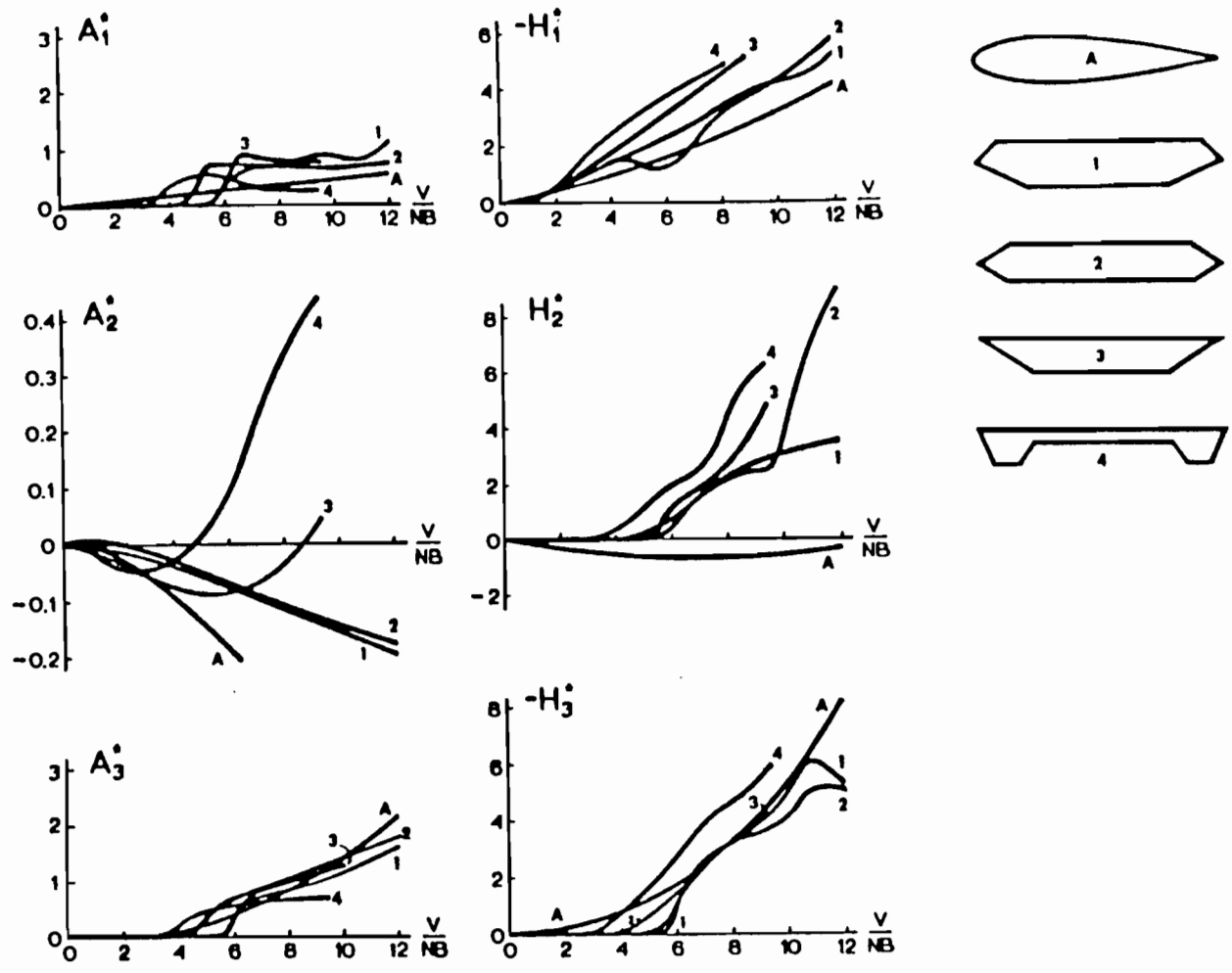
Figure 7.1 Flutter Derivatives of a Few Bridge Cross Sections
(Scanlan 1978)

59
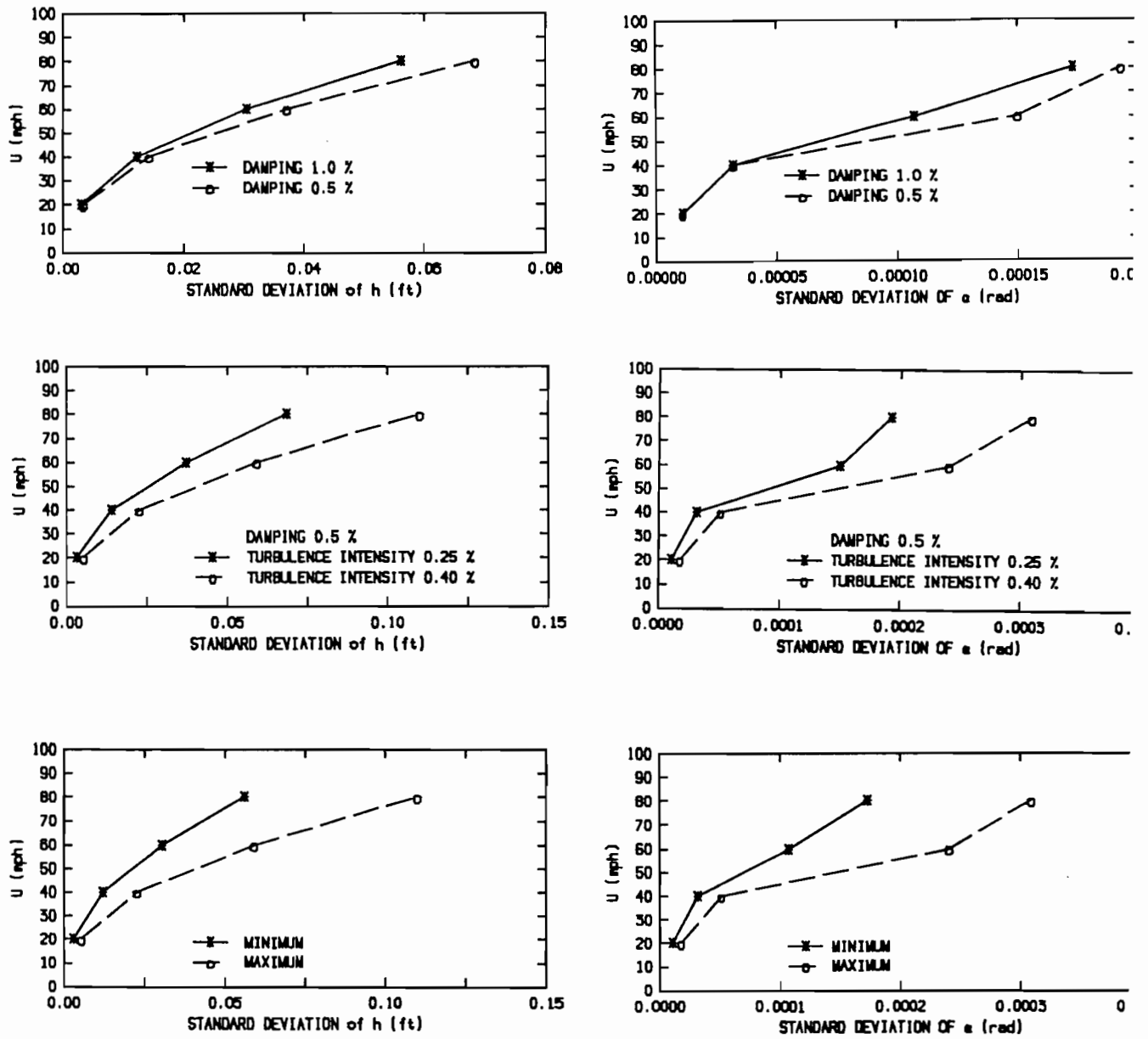
Figure 7.2 Buffeting Response of the Deck
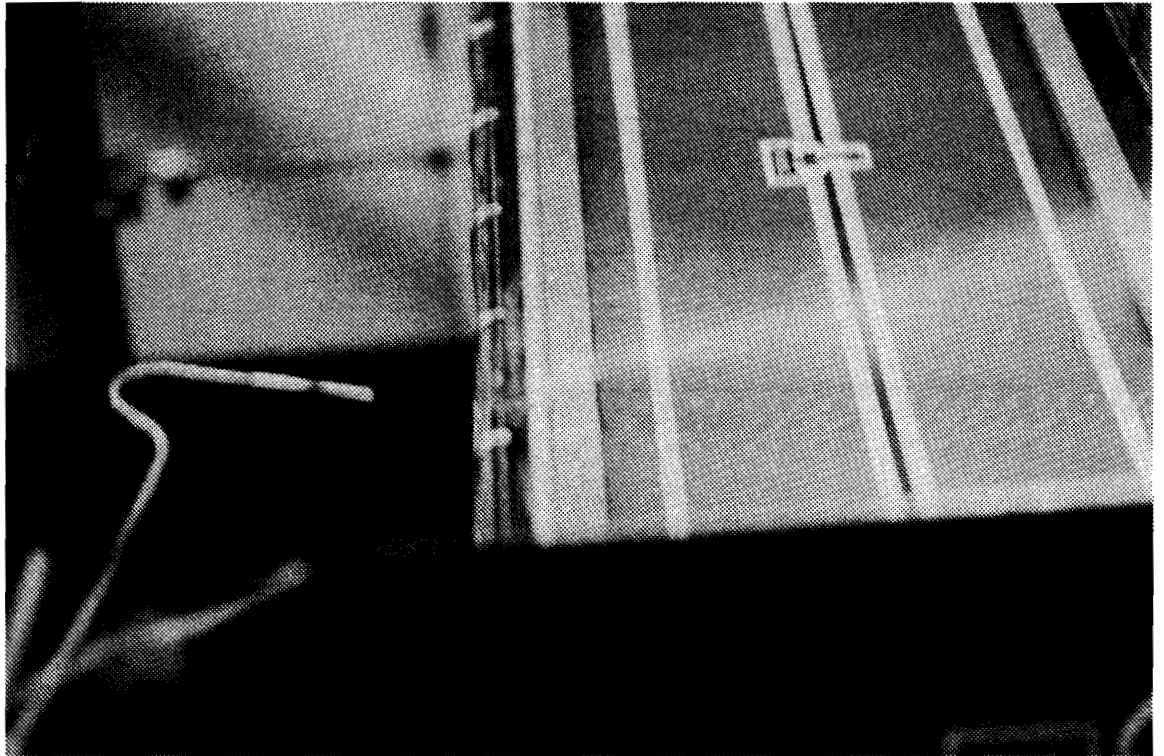
60
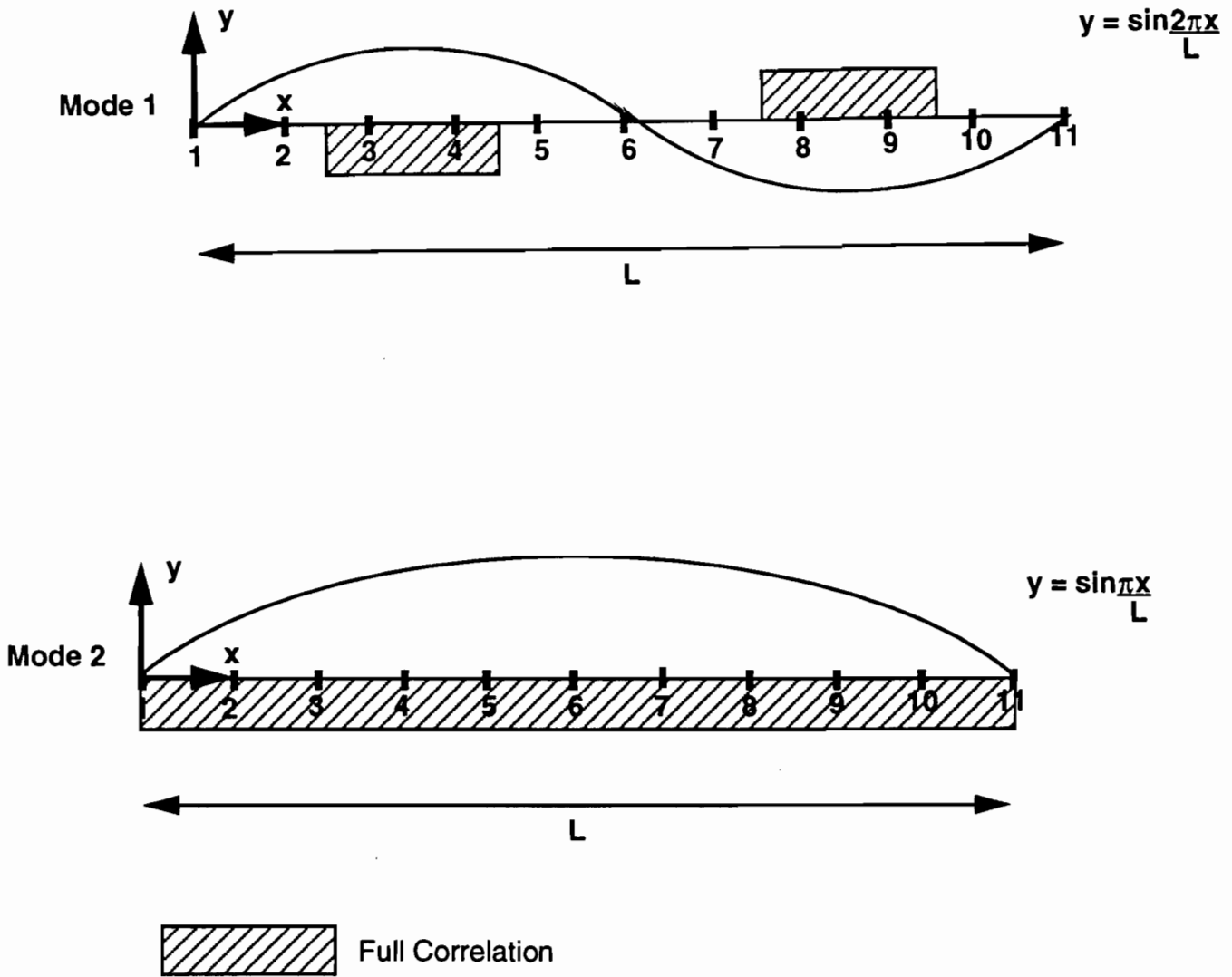
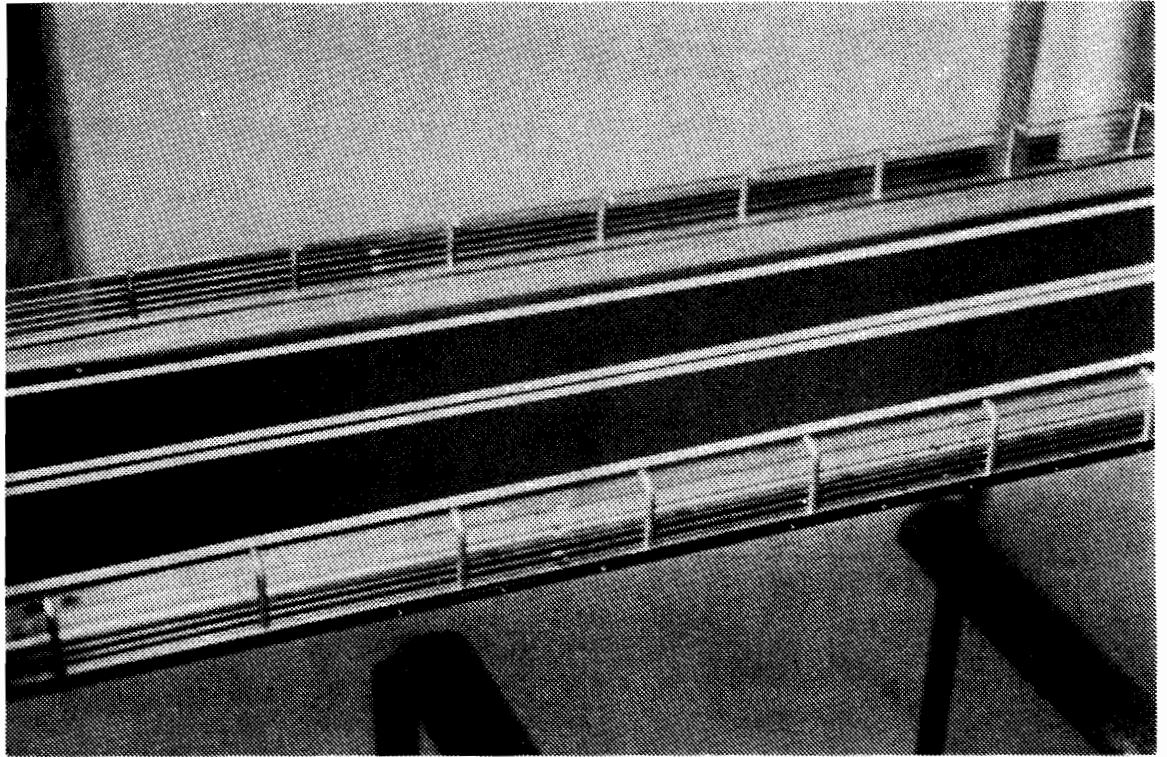Figure 7.3 Span-wise Correlation of Vortices Shed from the Deck

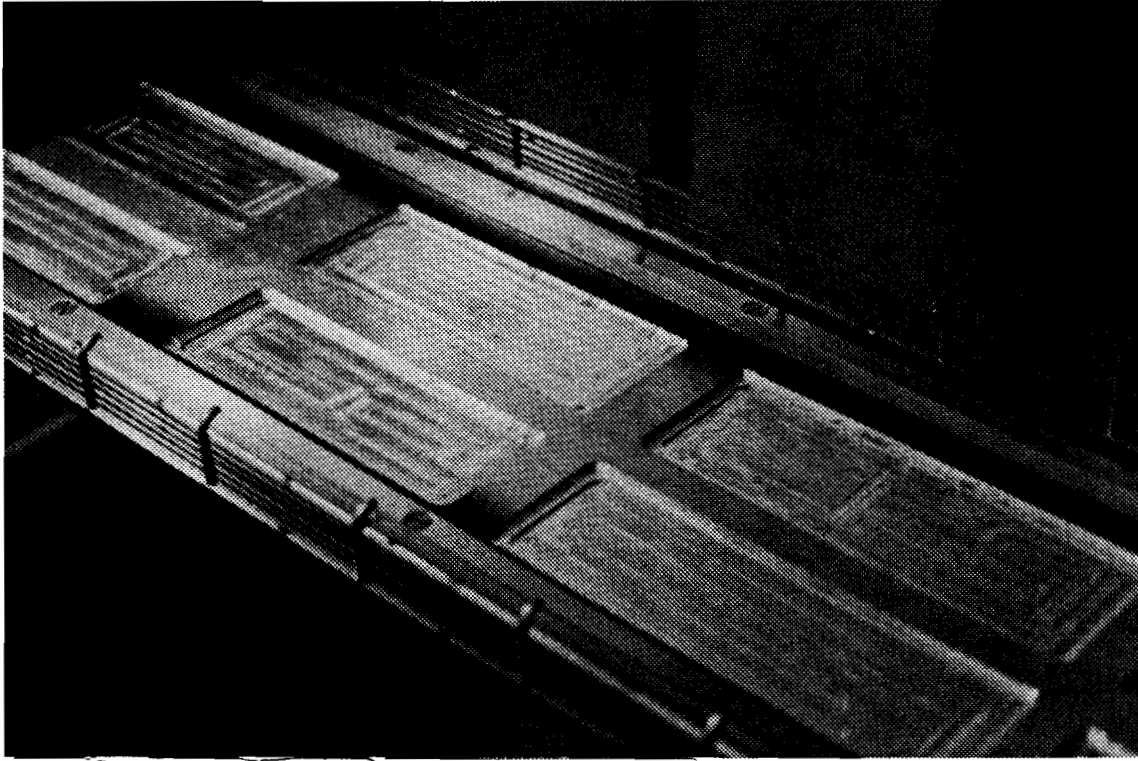Figure 7.4 Photographs showing Details of the Section Model

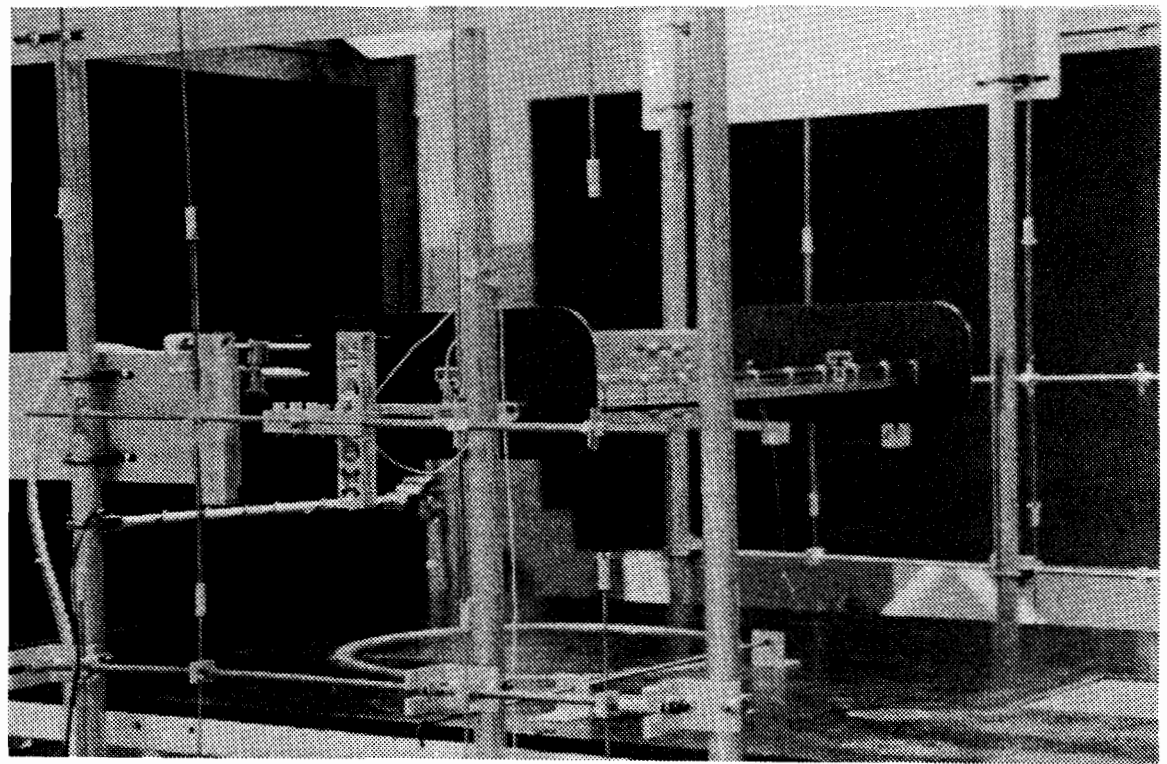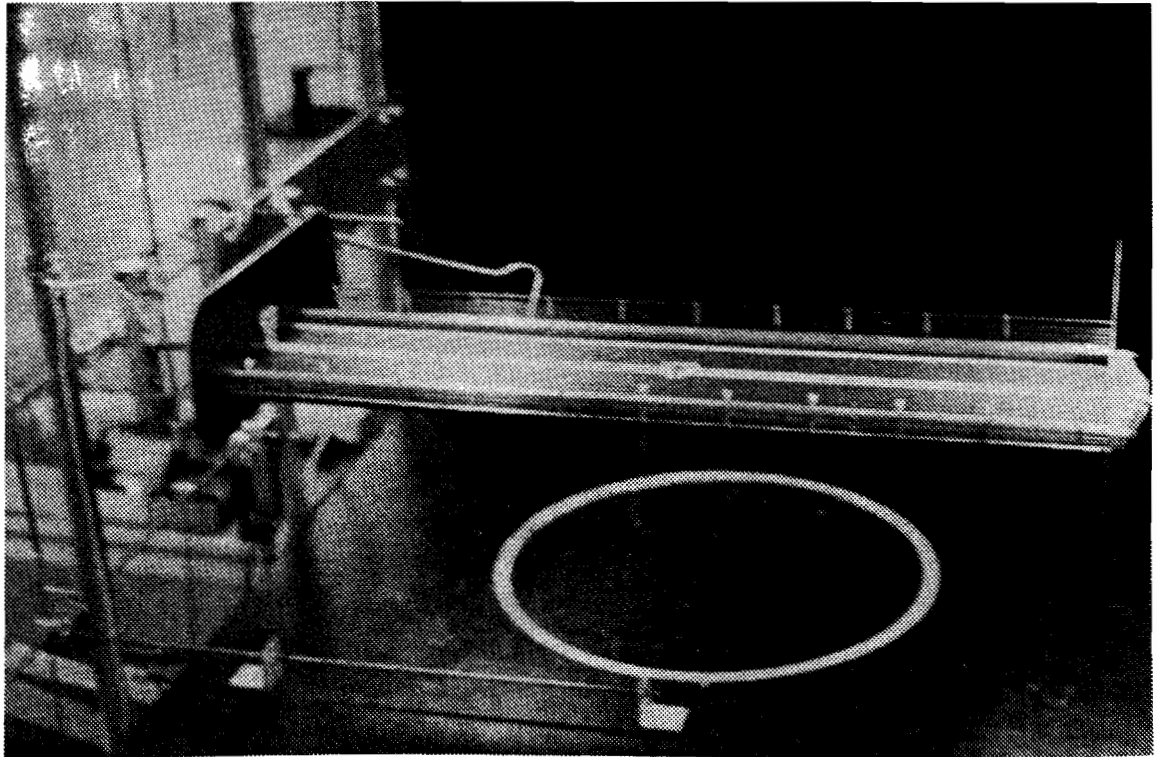Figure 7.5 Hollowed out Aluminum Block for the Section Model

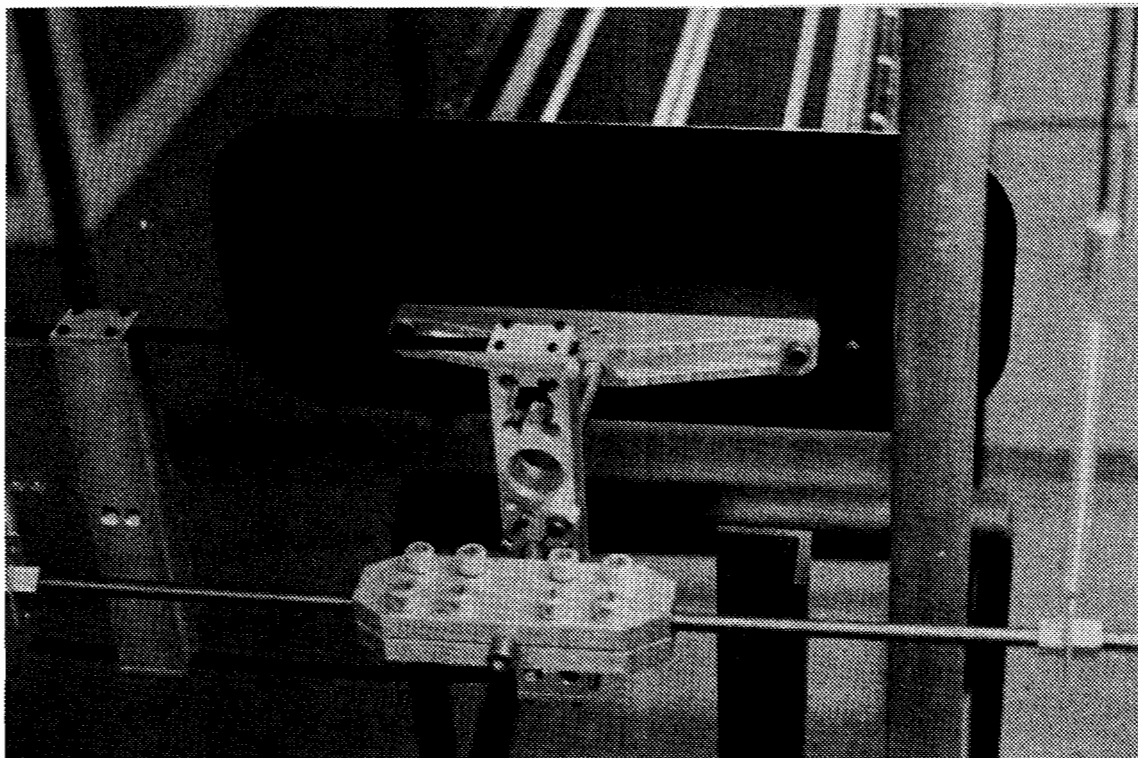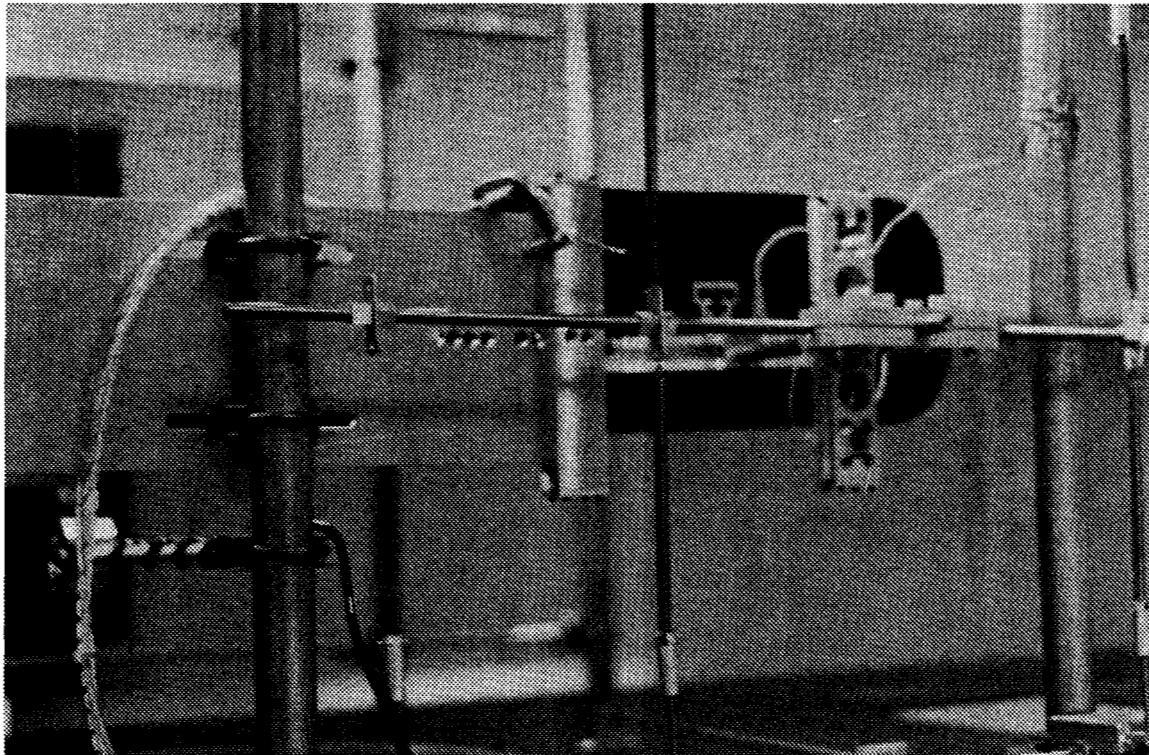Figure 7.6 Photographs of the Suspension System

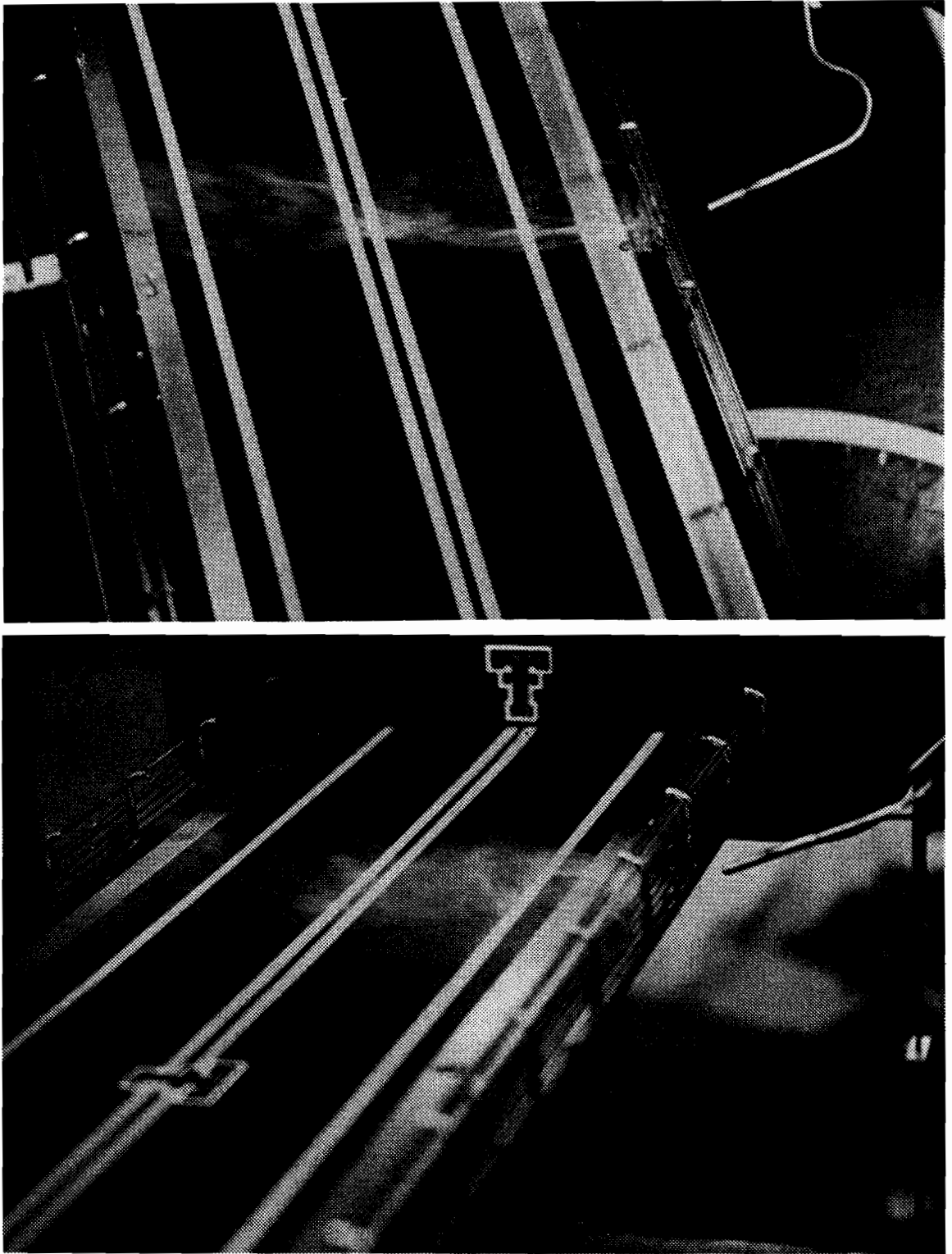Figure 7.6 Photographs of the Suspension System (continued)

Figure 7.7 Flow Visualization of Vortices with Smoke

APPENDIX C
(Vortex-Induced Response of Deck Hangers)

The formula for calculating the frequency of vibration ω (rad/s) of a hanger having mass per unit length m and length L and carrying a tensile load T is given by

$$\omega = \frac{n\,\Pi}{L}\sqrt{\frac{T}{m}}, \quad n = 1,2,3... = \text{mode number} \tag{9}$$

The above formula is modified if the flexural rigidity EI of the hanger is included in the calculation of frequency. The modified formula is

$$\omega = \frac{n\,\Pi}{L}\sqrt{\frac{n^2\Pi^2 EI}{mL^2} + \frac{T}{m}}, \quad n = 1,2,3... = \text{mode number} \tag{10}$$

When EI is negligible, Eqn. 10 takes the same form as Eqn. 9. The corresponding mode shapes of the hanger are

$$\Phi_n(x) = A \times \text{Sin}(\frac{n\,\pi\,x}{L}), \quad n = 1,2,3... = \text{mode number} \tag{11}$$

The following values are used for calculating the fundamental frequency of the hanger located at the center of the span (hanger no. 5)

$m =$ mass per unit length $= 5.55$ lb/ft $= 0.014$ slugs/in. (81.0 N/m)
$T =$ Tensile Force $= 74.2$ kips (330.1 kN)
$L =$ Length $= 32.5$ ft (9.91m)
$A =$ Metallic Area $= 1.59$ in.^{2} (1025.8 mm^2)
$D =$ Equivalent diameter based upon $A = 1.42$ in. (36.1 mm)
$E = 24 \times 10^6$ psi (1.65×10^8 kPa)
$I = \pi D^4/64 = 0.20$ in.^{4} (8.32×10^4 mm^4)

The frequencies (f_n) calculated for hanger 5 using Eqn. 9 and Eqn. 10 are 10.22 Hz and 10.25 Hz, respectively. It is decided to use Eqn. 9 for all the hangers because the frequencies calculated using Eqn. 10 differed very slightly from those calculated using Eqn. 9.

The Strouhal number (St) of any cross section is defined as follows

$$St = \frac{f_s\,D}{U} \tag{12}$$

where f_s is the frequency of vortex shedding, D is a characteristic dimension perpendicular to the flow, and U is the mean wind speed.

68

When the vortices are shed at a frequency which matches with one of the natural frequencies of the hanger, then the hangers tend to be excited. The corresponding mean wind speed (U) is called the lock-in speed at which this phenomenon will occur and can be calculated using Eqn. 12 where f_n is used instead of f_s.

The Strouhal number (St) of a circular cross section is 0.2 for Reynolds number $(\Re)$ of 500 to 10^4. There are two hangers in a side-by-side configuration in each set of hangers. The ratio of the distance between hangers $(E = 12$ in. or 305 mm$)$ to the diameter $(D = 1.625$ in. or 41.28 mm$)$ of each hanger is 7.4. It is known that as long as E/D is greater than 4.0, the vortices shed from one hanger will not interfere from those shed by the other hanger. Hence, St does not need to be modified.

Using Eqn. 12, $U = f_n D/St = 10.22 \times 1.625/(0.20 \times 12) = 6.92$ ft/s $(2.11$ m/s$)$ is the lock-in speed for hanger number *five* in its first mode. Similarly, the lock-in speed for each hanger is calculated and tabulated in Table 7.4.

The amplitude of vibration at lock-in wind speed can be calculated using the following formula

$$Y(x) = D\xi_o \Phi(x) \tag{13}$$

in which

$$\xi_o = \frac{2}{\sqrt{\epsilon}}\sqrt{\frac{\phi_2}{\phi_4}}\left[1 - \frac{4\pi m \zeta St}{\rho D^2 Y_1}\right]^{1/2} \tag{14}$$

where considering only the first mode shape $\Phi(x) = \text{Sin}(\frac{\pi x}{L})$, $\phi_2 = \int \Phi^2(x)\frac{dx}{L}$ and $\phi_4 = \int \Phi^4(x)\frac{dx}{L}$, ζ is the critical damping ratio, ρ is the air density, and Y_1 and ϵ are experimentally obtained parameters.

If it is assumed that vortices are fully correlated over the whole length of the hanger, then $\phi_2 = 0.500$ and $\phi_4 = 0.375$. The parameters Y_1 and ϵ are taken as 4.96 and 624.0, respectively, for a circular cross section (Goswami 1991). Assuming a damping ratio (ζ) of 0.02%, Eqn. 13 gives the value of the amplitude of steady-state vibration $Y_{max} = Y(L/2)$ at the mid height of the hanger as 0.12 in. $(3.05$ mm$)$.

The same calculation can be repeated by assuming that vortices are correlated only over the middle third of the length of the hanger. The amplitude of vibration for this case is 0.10 in. $(2.54$ mm$)$.

69